UNIVERSITY OF CALIFORNIA SAN DIEGO

Minimally Invasive Continuous Ketone Monitoring using Electrochemical Microneedle Biosensor

A Thesis submitted in partial satisfaction of the requirements
for the degree Master of Science

in

Bioengineering

by

Aishwarya Balaje

Committee in charge:

Professor Joseph Wang, Chair
Professor Gert Cauwenberghs, Co-Chair
Professor Pedro Cabrales

2024

The Thesis of Aishwarya Balaje is approved, and it is acceptable in quality and form for publication on microfilm and electronically.

University of California San Diego

2024

DEDICATION

To my kind, loving and supportive family.

TABLE OF CONTENTS

LIST OF FIGURES

LIST OF ABBREVIATIONS

3BHB	3-β-hydroxybutyrate
AA	Ascorbic Acid
AC	Azure C
AcAc	Acetoacetate
AcAc-CoA	Acetoacetyl-coenzyme A
Acetyl-CoA	Acetyl-coenzyme A
AD	Alzheimer's Disease
AI	Artificial Intelligence
AP	Acetaminophen
ATP	Adenosine Triphosphate
Au	Gold
BBB	Blood-Brain Barrier
BHB	β-hydroxybutyrate
CGM	Continuous Glucose Monitoring
Chit	Chitosan
CKM	Continuous Ketone Monitoring
CNS	Central Nervous System
CNT	Carbon Nanotubes
CPT-1	Carnitine Palmitoyl Transferase
DKA	Diabetic ketoacidosis
DLP	Digital Light Processing

DM	Diabetes mellitus
ECG	Electrocardiogram
FFAs	Free-fatty acids
Glu	Glucose
HBD	β-hydroxybutyrate Dehydrogenase
HMG-CoA	3-hydroxy-3-methylglutaryl-Coenzyme A
ISF	Interstitial Fluid
KBs	Ketone Bodies
KD	Ketogenic diet
Lac	Lactate
LCD	Low-carbohydrate diet
MB	Methylene Blue
MeB	Meldola Blue
Med ()	Mediator
MG	Methylene Green
MN	Microneedle
NAD^+	Nicotinamide Adenine Dinucleotide
NADH	Nicotinamide Adenine Dinucleotide Hydrate
NADPH	Nicotinamide adenine dinucleotide phosphate
NBA	Nile Blue A
PBS	Phosphate Buffer Solution
PD	Phenanthroline Dione
POC	Point-of-Care

Poly-TBO	Polymerized Toluidine Blue O
Pt	Platinum
PVC	Poly(vinyl chloride)
RE	Reference Electrode
SPCE	Screen-Printed Carbon Electrodes
T1DM	Type 1 diabetes mellitus
T2DM	Type 2 diabetes mellitus
TAGs	Triacylglycerols
TBO	Toluidine Blue O
TCA	Tricarboxylic Acid Cycle
UA	Uric Acid
UV	Ultra-Violet
WE	Working Electrode

ACKNOWLEDGEMENTS

I would like to deeply thank my advisor professor Joseph Wang for his exceptional support, guidance, and trust throughout the course of my Masters. Prof. Wang's dedication to the advancement of this field consistently shifts my perception of what all is possible in the scope of science and engineering. Also, I'd like to thank my committee members, Prof. Gert Cauwenberghs and Prof. Pedro Cabrales, for their guidance throughout this journey.

I've been privileged to receive exceptional support, knowledge, and dedicated teamwork from Dr. Chochanon Moonla, which made the success of our projects a joyful journey. I appreciate the opportunity to work with exceptionally talented member of our lab, especially Amal Abbas, Maria Reynoso, and Dr. Kuldeep Mahato for their undivided support in developing systems required for the success of our microneedle-based wearable sensors platform. I'd like to acknowledge the direct/indirect teamwork, support, and contributions of my coauthors; Chochanon Moonla, Amal Abbas, Maria Reynoso, Kuldeep Mahato, An-Yi Chang, Zhengxing Li, Omeed Djassemi, Ana Casanova.

Finally, I'd like to express my deepest gratitude to my loving family. My success throughout the Master's program truly stems from their love, care, and support that I've been privileged to receive.

VITA

2019 B.S. in Electronics and Communication Engineering, SRM University, India

2024 M.S. in Bioengineering, University of California San Diego, USA

PUBLICATIONS

Abbas, A., Sage-Sepulveda, J. S., Siddiqui, M., Ondes, B., Balaje, A., Mahato, K., and Wang, J. (2024). A Daily Multi-Segment Capsule for Time-controlled Drug Release. Manuscript submitted for publication.

Moonla, C., Reynoso, M., Casanova, A., Chang, A.-Y., Djassemi, O., Balaje, A., Abbas, A., Li, Z., Mahato, K., and Wang, J. (2024). Continuous Ketone Monitoring via Wearable Microneedle Patch Platform. ACS Sensors, 9(2), 1004–1013. https://doi.org/10.1021/acssensors.3c02677

Praveenkumar S., Balaje A., Banerjee A., Induvalli, Sharma S., Jaya T. (2020). Simulation of Quantum Channel and Analysis of its State under Network Disruption. Advances in Intelligent Systems and Computing. Springer, vol. 1056, pp. 593-602. https://doi.org/10.1007/978-981-15-0199-9-51

FIELD OF STUDY

Major Field: Bioengineering

Studies in Bioengineering

Professor Joseph Wang

ABSTRACT OF THE THESIS

Minimally Invasive Continuous Ketone Monitoring using Electrochemical Microneedle Biosensor

by

Aishwarya Balaje

Master of Science in Bioengineering

University of California San Diego, 2024

Professor Joseph Wang, Chair
Professor Gert Cauwenberghs, Co-Chair

Diabetes is one of the fastest-growing chronic diseases worldwide, with diabetic ketoacidosis (DKA) significantly increasing the risk of complications and comorbidities. Effective diabetes management relies on accurate and timely blood glucose and ketone levels monitoring. Yet, traditional methods like frequent finger-prick blood tests or urine tests are invasive,

inconvenient, and often delay the detection of critical metabolic changes. This thesis explores the development of a Continuous Ketone Monitoring (CKM) system using an electrochemical microneedle biosensor. Ketone bodies, specifically β-hydroxybutyrate, are a key indicator of metabolic state and disease progression in diabetes. This work focuses on developing and validating a novel microneedle sensor capable of continuous, real-time monitoring of ketone levels directly from the interstitial fluid by building on the principle of electrochemical sensing, biocatalytic reactions, and microfabrication. The CKM system offers a minimally invasive, real-time alternative to traditional monitoring methods, by addressing many of their limitations and advancing it by proposing enhancements to overcome these challenges such as mediator leaching, HBD/NAD^+ immobilization, minimally invasive ISF BHB testing, and on-body testing. The sensor's performance was evaluated through a series of experiments, including in vitro and on-body tests, indicating promising accuracy and reliability compared to existing methods. By providing continuous feedback on ketone levels, CKM technology has the potential to significantly improve diabetes management, prevent DKA, and enhance patient compliance and quality of life. The study offers critical insights into their potential impact on the future of diabetes care. The findings suggest that this technology could represent a significant leap forward in the pursuit of improved diabetic health monitoring and management.

Chapter 1 Introduction

1.1 Ketone Bodies (KBs)

Ketone bodies (KBs) and ketosis have received tremendous attention lately due to their significant contribution to human health and disease monitoring, nutrition, and wellness [1] [2]. In recent decades, it has become evident that KBs are indicators of metabolic conditions of the body and disease status [1]. This makes sense as ketones are used as an alternate source of energy in our body. They were first detected in the urine of a type 1 diabetes mellitus (T1DM) patient [3]. This created an association of these ketone bodies to this deadly condition and hence were labeled as potential pathogenic markers for the last 100 years. Under normal conditions, the body relies on glucose as its primary source of energy, which is typically derived from carbohydrates, such as sugars, starchy foods, and grains. The body breaks these carbohydrates down into simple sugars, then either uses it up as glucose for immediate energy or stores them as glycogen in the liver and muscles for future use. In cases of insufficient glucose availability to meet the body's energy demands, it switches to an alternative method.

Ketosis is a metabolic state where your body doesn't have enough carbohydrates to burn for energy, from the low-carb Keto diet [4] [5]. Instead, it burns fat and makes ketones (as seen in Figure 1). KBs are produced in the body by the liver during periods of high caloric restrictions (low food intake, fasting low-card diets, strenuous exercise, etc.), primarily to sustain memory formation, but also during periods of starvation, alcoholism, and disease status (untreated type 1 diabetes mellitus, hyperemesis gravidarum, heart and Alzheimer's diseases (AD), and various metabolic disorders) [6]. The body begins breaking down fat stores and converts triglycerides to

glucose. This metabolic shift (ketosis) is characterized by ketonemia and ketonuria, which is the accumulation of these acids in the blood and excretion through urine [7] [8].

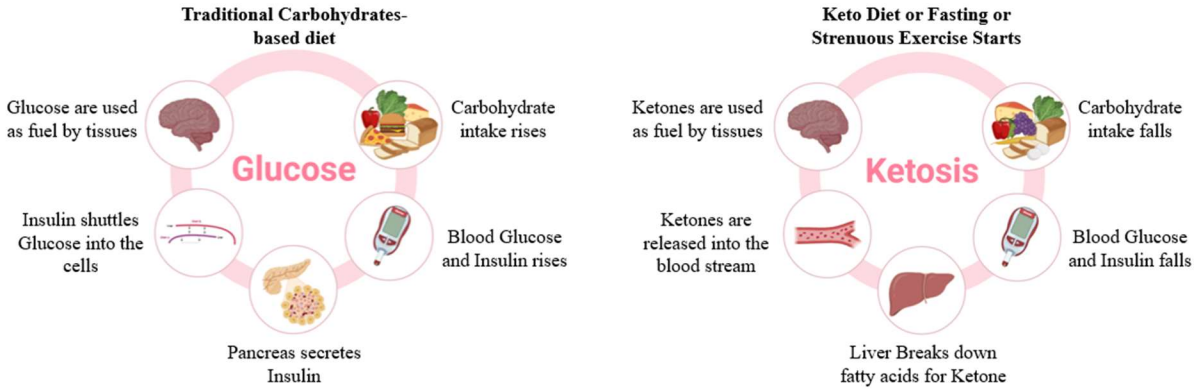

Figure 1: Glucose (Carbohydrates-based diet) vs Ketone (Keto diet) as source of energy.

Functionally, the body produces two primary ketone bodies, acetoacetate (AcAc) and β-hydroxybutyrate (BHB), which are crucial in energy metabolism and biological process signaling. AcAc is the first ketone body produced during the breakdown of the free fatty acids in the liver, a process known as ketogenesis. Once synthesized, AcAc can follow one of the two pathways: AcAc can be converted into acetyl-CoA, which then enters the citric acid cycle (Krebs cycle) to produce ATP, or it can be reduced to BHB (as seen in Figure 2), a process that occurs in response to the body's cellular redox state (the balance of NAD^+/NADH). This conversion is particularly significant in periods of high-fat metabolism, such as fasting or prolonged exercise [9]. A higher ratio suggests a more reduced environment (higher NADH levels), which can influence metabolic pathways and signal the body to adapt to changes in energy availability. BHB is the more reduced form of acetoacetate and is often present in higher concentrations during states of ketosis. It provides an efficient and readily available source of energy for tissues such as the brain, heart, and muscles, especially when glucose availability is low [2]. Unlike free fatty acids, KBs can cross the blood-brain barrier (BBB) and hence, are also available as fuels for the CNS cells.

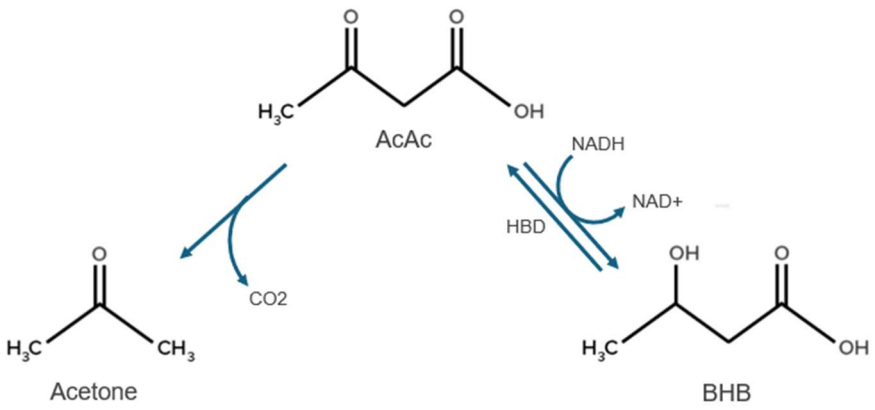

Figure 2: Acetoacetate conversion to Acetone and beta-hydroxybutyrate (BHB) [10] [11] [12]

In small quantities, ketones indicate that fat is being metabolized. However, elevated levels of ketones can be harmful, potentially leading to a dangerous condition known as ketoacidosis. In ketoacidosis, the overproduction of ketones results in their accumulation in the blood, causing the blood to become overly acidic. This acidification can disrupt normal bodily functions and, if not addressed, can lead to severe complications.

A particularly severe form of ketoacidosis is Diabetic Ketoacidosis, also known as DKA, which occurs predominantly in people with diabetes, particularly T1DM. It occurs when there is a severe insulin deficiency, leading to high blood sugar levels and forcing the body to break down fat at a rapid pace, producing large amounts of ketones [13]. Primarily affects individuals with type 1 diabetes, but it can also occur in people with type 2 diabetes under certain conditions, such as during periods of illness or severe stress. DKA is a life-threatening complication of both Type 1 and Type 2 Diabetes Mellitus (T2DM), which if left untreated can lead to coma and death.

1.2 Need for BHB Monitoring: Diabetes and Ketoacidosis

At the core of DKA is diabetes, a chronic condition that is rapidly becoming one of the most prevalent diseases globally. It is a major contributor to illness, disability, and early death,

with the risk of developing cardiovascular diseases increasing by 2 to 4 times in those with diabetes [14] [15] [16]. In 1980, 108 million people worldwide had diabetes, a number that surged to 422 million by 2014, according to the World Health Organization [17]. As seen in Figure 3, China currently has the highest number of diabetes cases, with 116 million people affected, followed by India with 77 million, and the United States with 31 million [18]. In the United States, estimates for 2021 show that of the 31 million people who were diagnosed with diabetes, 352,000 were children and adolescents under 20 years old, of whom 304,000 have type 1 diabetes [19]. Additionally, 97.6 million adults aged 18 or older were estimated to have prediabetes in 2021 [20]. Alarmingly, an American is diagnosed with diabetes every 17 seconds [21].

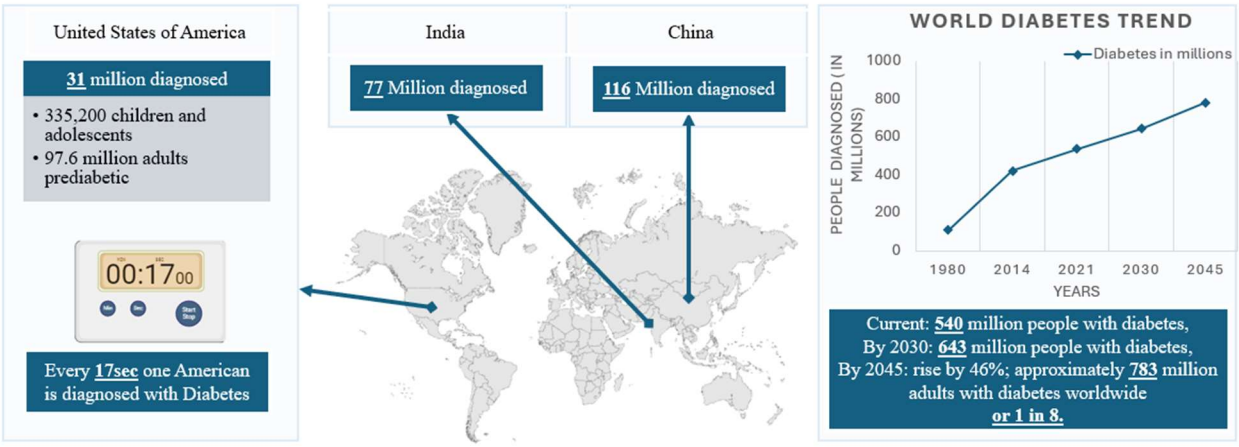

Figure 3: Diabetes statistics (Worldwide and USA)

Currently, there are 540 million people with diabetes worldwide, and projections by the IDF suggest that by 2045, this number could rise by 46%, affecting approximately 783 million adults, or 1 in 8 [22]. Diabetes disrupts the body's ability to regulate blood sugar levels, often leading to hyperglycemia. In cases where insulin levels become critically low or absent, as in type 1 diabetes, the risk of developing DKA significantly increases. Therefore, understanding and managing diabetes is crucial not only for preventing hyperglycemia but also for reducing the risk of DKA and other serious complications associated with the kidney, liver, and heart.

DKA has been observed to have higher prevalence rates among women and non-White populations. Studies in the USA and Europe have shown ever-increasing hospitalizations for DKA in adults with a 1.1% DKA hospitalization rate from 2000 to 2009 to 6.3% from 2009 to 2014 [1] [23]. In Europe, data from the DPV registry indicated that adults with T1DM had a DKA rate of 2.5 per 100 patient-years. A 2020 U.S. study identified 220,340 T1DM patients with a primary diagnosis of DKA, with a mean age of 38.4 years; 53.3% were between 18 and 44 years old. DKA is particularly common among children and adolescents with T1DM, leading to increased hospitalizations, recurrence, and mortality. Younger children are especially at risk for DKA at the time of T1D diagnosis, as the symptoms may go unrecognized. From 2010 to 2016, the prevalence of DKA in the United States increased from 35.3% to 40.6%, with a 2% annual rise in cases of DKA at or near the time of T1D diagnosis. The prognosis for DKA worsens significantly at the extremes of age, particularly with the occurrence of coma, hypotension, and severe comorbidities. Mortality rates exceeding 5% have been reported among the elderly and those with life-threatening illnesses. In the U.S., a study found that nursing home residents accounted for 0.7% of DKA cases, with increased mortality associated with this population [23]. The geriatric population is especially at risk for developing hyperglycemic crises due to factors like increased insulin resistance and decreased thirst mechanisms. The elderly are particularly susceptible to hyperglycemia and dehydration, which are critical components of hyperglycemic emergencies. However, with enhanced diabetes surveillance and aggressive early treatment of hyperglycemia and its complications, morbidity, and mortality from acute diabetic crises in the elderly can be significantly reduced.

Given the risks associated with ketoacidosis, monitoring ketone levels to prevent, diagnose, and treat diabetic ketoacidosis (DKA) becomes crucial, especially for individuals with diabetes

who are at higher risk. Regular ketone monitoring allows for early detection of rising ketone levels, enabling timely intervention before the condition progresses to ketoacidosis. Traditionally, ketone levels are monitored using urine strips or blood tests, but these methods come with several significant limitations that can impact the effectiveness of diabetes management. More importantly, they are often used only after symptoms have been prevalent. There is no real-time monitoring which limits the ability to react proactively to the rising ketone levels in the blood or in the urine. Having to rely on symptoms like fruity-smelling breath, thirst, a very dry mouth or frequent urination to determine whether there is a need to test the blood ketone or ketone in urine, is not very efficient for early detection of ketone buildup, and in the long run not ideal or consistent practice for most patients.

To enhance diabetes management and prevent complications like DKA, there is a growing need for Continuous Ketone Monitoring (CKM). The development of minimally invasive CKM technologies represents a significant advancement in diabetes care [24] [25] [26]. CKM provides accurate, real-time data on ketone levels, offering a more dynamic and proactive approach to monitoring with minimum discomfort. With CKM, individuals can track ketone trends continuously, allowing them to make informed decisions about their insulin dosing, diet, and activity levels. This continuous feedback loop is particularly valuable in preventing the onset of ketoacidosis by alerting users to rising ketone levels before they become dangerous. Unlike traditional methods that require frequent finger pricks or urine sampling, minimally invasive CKM devices use technologies such as microneedle patch sensors to continuously monitor ketone levels in the interstitial fluid [27] [28] [29]. These devices are designed to be discreet, easy to use, and integrated with other diabetes management tools, making them an attractive option for individuals seeking to optimize their health and prevent complications.

Given the critical need for continuous and reliable monitoring of ketone levels in diabetes management, my thesis delves into the development and applications of minimally invasive Continuous Ketone Monitoring (CKM) technology using an electrochemical microneedle sensor. This innovative approach aims to provide a minimally invasive, real-time solution for tracking ketone levels, enhancing the ability to prevent diabetic ketoacidosis, and improving overall diabetes care. By leveraging the latest advancements in electrochemical sensors and microneedle technology, this platform represents a significant step forward in the field of digital health and wearable medical devices. My thesis explores minimally invasive CKM technology, the fabrication and enzymatic modifications of the electrochemical microneedle-based biosensors, the underlying principles of biocatalytic reactions on the sensor surface, electrochemical analysis, in-vitro detection and measurement of NADH and BHB, on-body testing capabilities, potential implications, and future directions of CKM using this cutting-edge sensing technology.

Chapter 2 Related Works and Background

2.1 Conventional Ketone Detection

The incredible pace at which technological advancements have happened over the past few decades has impacted our lives in more ways than we can count. Especially in the field of healthcare and biological sciences. The healthcare sector is going through rapid transformations which impact both patient care and operations. These advancements in healthcare have revolutionized the way medical services are delivered and how medical data is managed, improving patient outcomes, enhancing the efficiency of healthcare, and expanding the capabilities of diagnostics, treatment, and patient monitoring. Over the past few decades, we have seen the world collectively move towards one goal – to improve global quality of life through better patient care, public health, and reduced costs. We have seen advancements in genomics and personal medicine, robotics in surgery, advanced imaging technology, CRISPR and gene editing, regenerative medicine, telemedicine and telehealth, AI, and finally wearable health technology. These advancements not only enhance the quality of care but also make healthcare more personalized and efficient, making strides toward a future where medical treatment is more responsive to individual needs and global health challenges.

On that note, one of the first things we learn growing up is “prevention is better than cure.” This has now become the fundamental principle of modern healthcare across the world. Securing global healthcare will require significant and sustained efforts to prevent illness and support good health, both physical and mental. The first thought that naturally comes to mind is diagnostics and patient monitoring. Biomedical diagnostics, a critical aspect of healthcare, has seen significant advancements in transitioning from invasive, blood-based methods typically confined to hospital settings to more personalized, decentralized, and remote diagnostic approaches. This evolution is

particularly evident in the detection of ketone bodies (KBs), where advancements in small-scale electrochemical sensing methods have enabled more accessible and timely monitoring.

As mentioned in the introduction, historically, KBs were measured using blood and urine samples, with urine testing for acetoacetate (AcAc) and blood testing for β-hydroxybutyrate (BHB). However, there is delayed detection as seen with the urine strips measuring the amounts of ketone excreted in the urine, which reflects ketone levels from several hours earlier. This delay in detection can prevent timely intervention, increasing the risk of DKA before the patient is even aware of rising ketone levels. The introduction of the first colorimetric paper-based ketone detection strip in 1984 and the subsequent development of a dry-strip electrochemical sensor by Batchelor et al. in 1988 marked significant milestones in the journey toward more efficient ketone monitoring [30] [31]. This was a simple electrochemical sensor with a redox mediator (4MQ) layer and a layer dependent on a dehydrogenase enzyme derivative and NAD^+ cofactor. In 1999, Stewart et al. introduced a dual electrochemical detection system for BHB and glucose, leading to a point-of-care (POC) device for BHB monitoring. This innovation was followed by the first commercial dual analyte (BHB/glucose) sensor strip by Medisense/Abbott Laboratories in 2000, validated against traditional urinary acetoacetate strips. Over the next decade or so, attempts were made to improve the sensor strip [32]. In 2008, printed film sensors were introduced which showed single-step BHB detection without the need for any mediator. In 2016, Whitesides's team developed an electrochemical paper-based device (pop-up-EPAD) for BHB detection, demonstrating comparable performance to plastic test strips in a commercial glucometer. In 2017, Guo introduced a smartphone-integrated electrochemical analyzer, providing a portable and accessible solution for point-of-care blood ketone monitoring (compiled in Figure 4) [33].

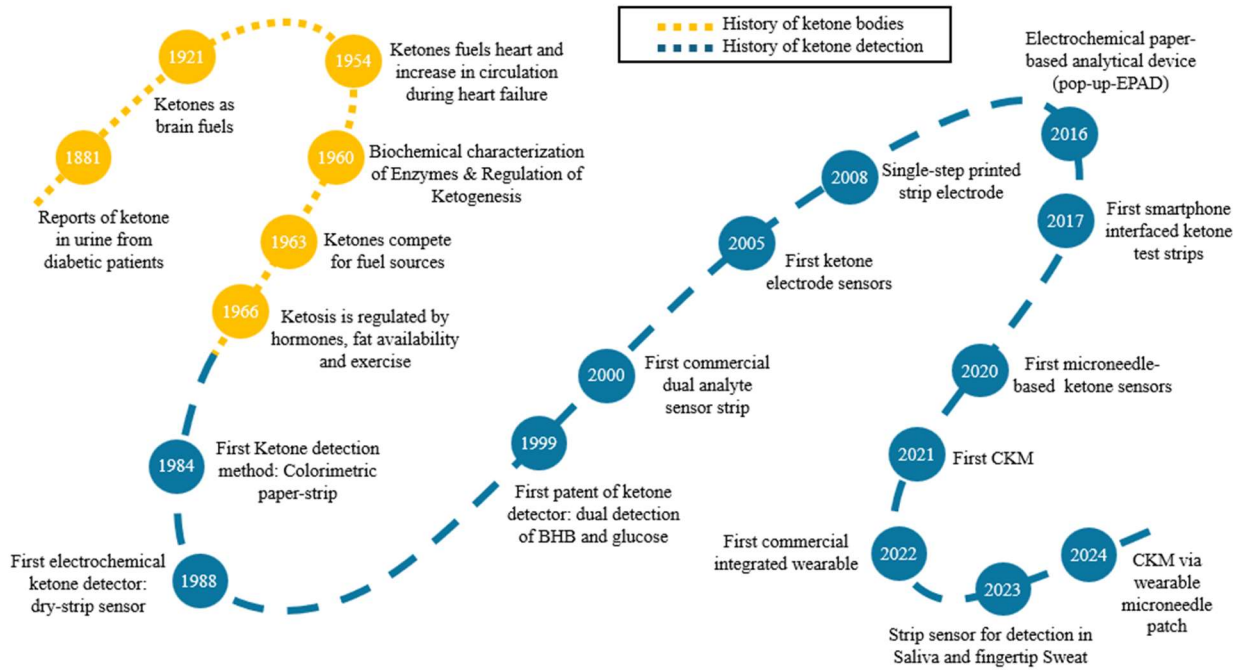

Figure 4: History of ketone body metabolism and ketone detection [3]

But there are numerous significant limitations associated with the conventional methods for ketone detection. Both urine and blood ketone tests are typically performed at specific times, often when symptoms arise, rather than continuously. This sporadic testing can miss fluctuations in ketone levels, leaving gaps in monitoring that can be critical in detecting the early onset of ketoacidosis. Blood ketone tests require frequent finger pricks, which can be painful and inconvenient, particularly for individuals who need to monitor their ketone levels regularly [33] [34]. This is like conventional diabetes management where monitoring blood glucose is typically done through frequent finger pricks to obtain blood samples, requiring patients to perform this invasive procedure multiple times daily, totaling around 1800 finger-pricks per year and 90,000 finger-pricks over a period of 50 years [35]. This repetitive process not only causes discomfort but also carries a risk of blood-borne infections associated with invasive ketone sensors. The discomfort associated with repeated testing often leads to poor compliance, with users less likely to test as frequently as needed.

2.2 Minimally Invasive Ketone Monitoring

Efforts have been made to develop minimally invasive or non-invasive ketone monitoring devices, utilizing various techniques. As a promising alternative, researchers are exploring methods to measure ketone concentrations in more easily accessible body fluids, such as the Interstitial Fluid (ISF), sweat, tear fluid, and saliva [36] [37]. Among these, sweat, tear fluid, and saliva were predominantly tested for creating a non-invasive monitoring platform. This was due to the ease of accessibility, as these methods do not require skin pricking. ISF is particularly advantageous because it is more readily accessible than blood, can be continuously collected, and is less prone to dilution (or dependent on hydration) compared to urine [38]. This approach has significant potential for non-invasive diabetes diagnosis and management. Although these methods still need to be frequently validated against direct blood ketone measurements in the testing phase, they have created a much sought-after avenue for the future.

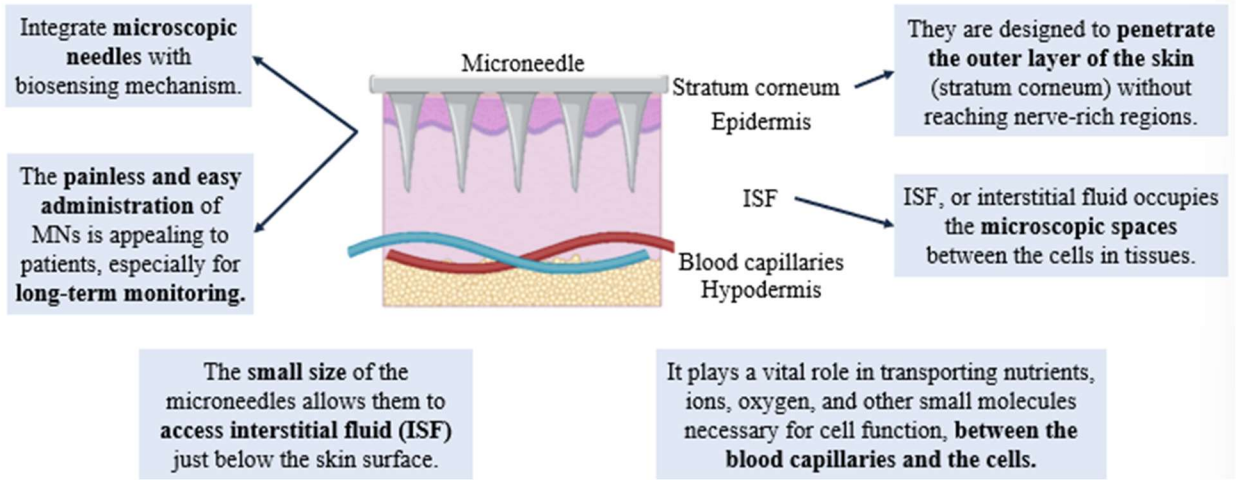

Figure 5: Microneedles for measurement in ISF

ISF, or interstitial fluid, is the fluid that occupies the microscopic spaces between the cells in tissues, also called the interstitial spaces (Figure 5). It is present between blood vessels and the

cells they supply and plays a vital role in transporting nutrients, ions, oxygen, and other small molecules, which are necessary for cell function, between the blood capillaries and the cells. It also carries carbon dioxide and waste products from the cells to the blood for removal from the body. Small molecules like glucose, oxygen, and electrolytes can freely pass through the capillary walls into the ISF, while larger molecules and proteins are typically restricted. The composition of ISF is maintained in equilibrium with the blood plasma, with constant exchange occurring to balance the levels of nutrients, gases, and waste products. This means that the concentration of glucose, ketones, and other metabolites in ISF closely reflects their levels in the blood. The only issue here is the small time lag associated with the maintenance of the equilibrium. Hence, ISF is a valuable medium for biomarker monitoring using continuous monitoring technology, as it can provide real-time insights into a patient's metabolic status without the need for direct blood sampling or urine sampling. These peripheral biochemical monitoring and electrochemical sensing methods offer minimally invasive measurement of metabolites in humans without ever breaking the endothelial barrier between capillaries and surrounding tissue cells.

This was a turning point in the field of biosensors. The first microneedle-based sensing approach for continuous BHB monitoring was introduced in 2020 by Teymourian et al., offering multiplexed detection of glucose and ketones in interstitial fluid (ISF), crucial for managing diabetic ketosis (DK) and diabetic ketoacidosis (DKA) [25]. In 2021, a new microneedle CKM system was introduced that demonstrated excellent analytical performance with a detection limit of 50 μM, effective even in the presence of potential interferences, paving the way for future applications in real-time, minimally invasive BHB monitoring. By the end of 2021, a commercial system integrating joint glucose and BHB monitoring was announced. 2022-2023 saw efforts focusing on detecting BHB in alternative body fluids, such as saliva and fingertip sweat, offering

rapid, decentralized, and painless detection methods. Despite their potential application, they have their own share of limitations, as in the case of sweat, the biofluid assessment and the volume collected would always pose an issue, as sweat is not as readily available in abundance as tear fluid or saliva. Recent efforts by the NBE group furthered ketone sensing and monitoring of saliva and sweat by demonstrating disposable screen-printed carbon electrodes (SPCE) for touch-based sweat analysis and measurement of salivary BHB, along with making strides in microneedle sensing platforms for ISF [39] [33] [37]. Recently, our team developed minimally invasive microneedle-based biosensors designed for monitoring various biomarkers in interstitial fluid (ISF), which is the focus of my thesis. Microneedle-based biosensors combine tiny, needle-like structures with technology originally developed for drug delivery, but they have recently been adapted for biosensing applications. These sensors are engineered to penetrate only the outermost layer of the skin, the stratum corneum, avoiding deeper, nerve-rich areas. This design makes them minimally invasive and virtually painless, which is particularly advantageous for patients who require long-term monitoring. The appeal of microneedles lies in their ease of use and pain-free application, making them an attractive option for continuous health monitoring [40]. The small size of these microneedles allows them to access interstitial fluid (ISF) just beneath the skin's surface. This enables the detection of important biomarkers, such as glucose, ketones, and other metabolites, without causing significant discomfort or skin damage. By providing a less invasive alternative to traditional methods, microneedle-based biosensors offer a promising solution for ongoing, real-time health monitoring, enhancing patient comfort and compliance. The minimally invasive nature of these microneedles enables pain-free biomarker monitoring with minimal tissue inflammation and promotes rapid skin recovery (compiled in Figure 4) [41] [25].

The concepts of “sense and act” and “minimally invasive” are revolutionizing the industry, one metabolite at a time. Smart CGM devices are the norm. These devices can sense blood glucose levels in real time and alert the user or automatically adjust insulin delivery through a connected insulin pump, effectively managing diabetes with minimal user intervention. The wearables now had sensing, data collection, data processing, and decision-making abilities along with the ability to take necessary actions (user alert, data sharing, or automatic adjustments). Wearable fitness devices were available in the market that can sense metrics like heart rate, sleep patterns, and physical activity. Based on the data, they can provide personalized recommendations, such as encouraging the user to move more or adjust their sleep routine. A smartwatch with an electrocardiogram (ECG) sensor can detect irregular heart rhythms (such as atrial fibrillation) and prompt the user to seek medical attention or automatically alert healthcare providers. A wearable microneedle patch could sense the body's need for a drug (like pain relief or insulin) and automatically deliver the appropriate dose through the skin, ensuring optimal treatment without user intervention or alerting the user of the body’s needs in times of low blood glucose levels or in our case elevated ketone levels.

2.3 Electrochemical Sensor for Ketone Monitoring

In the following sections, we will go over the electrochemical sensors, developed to monitor these ketone levels of the body continuously and effectively. But to understand the principles that govern the electrochemical sensor used for ketone monitoring, we first need to understand ketogenesis in the liver and ketone oxidation in the lungs, heart, and other extrahepatic tissues.

2.3.1 Ketogenesis and Ketone Oxidation

A normal circulating ketone level is lesser amounts of ketones in the blood, which are below 0.6 mmol/L (normal) [33]. This represents ~5% of total daily energy expenditure in a normal, healthy, fully fed, resting state. This fluctuates up to ~20% in starvation, alcoholism, strenuous exercise, or ketosis, which could be 0.6 to 1.5 mmol/L (low—moderate risk of DKA) where you would be advised to contact a healthcare provider, if persistent. Ketone levels of 1.6 to 2.9 mmol/L are high and would require you to seek medical attention (high risk of DKA) and levels above 3 mmol/L would require you to report to ER and seek urgent medical care (very high risk of DKA, prevalent ketonuria and ketoacidosis, and risk of coma or other complications) [42] [43]. To get this information, you could get a blood work-up done at your healthcare provider or buy a blood or urine self-testing kit at home. If you use strips to test for ketones in your urine and the result is over 2 mmol/L, it indicates high levels of ketones in the blood, which may suggest you have DKA. In this case, you should call emergency services or go to the nearest A&E immediately. This is where the importance of continuous monitoring of ketone is reiterated, as there are a lot of factors that could affect the result seen in the urine test. It is subject to the patient's dehydration level, fasting, or exercise, and there is a considerable time lag between the ketone level in blood and urine, which also increases the risk of not knowing if you have severe DKA before it is too late.

Under normal circumstances, our body derives energy from stored carbohydrates, and it breaks down glycogen to glucose and then glucose to pyruvate while generating ATP for the cellular process (as illustrated in Figure 6) [44] [45]. This process is called glycolysis. During periods of low glucose availability, the body tries to synthesize glucose from a non-carbohydrate source like lactate. This process is called gluconeogenesis, which is considered to be the reverse

of glycolysis, but with some key regulatory differences. During low glucose periods, oxaloacetate from the Krebs cycle will enter the gluconeogenic pathway, is removed from the mitochondria of the liver cells and is converted into glucose in the cytoplasm of liver cells and released into the blood. Oxaloacetate is a crucial metabolic intermediate that is involved in many important pathways, particularly the tricarboxylic acid cycle (TCA), also known as the Krebs cycle and gluconeogenesis.

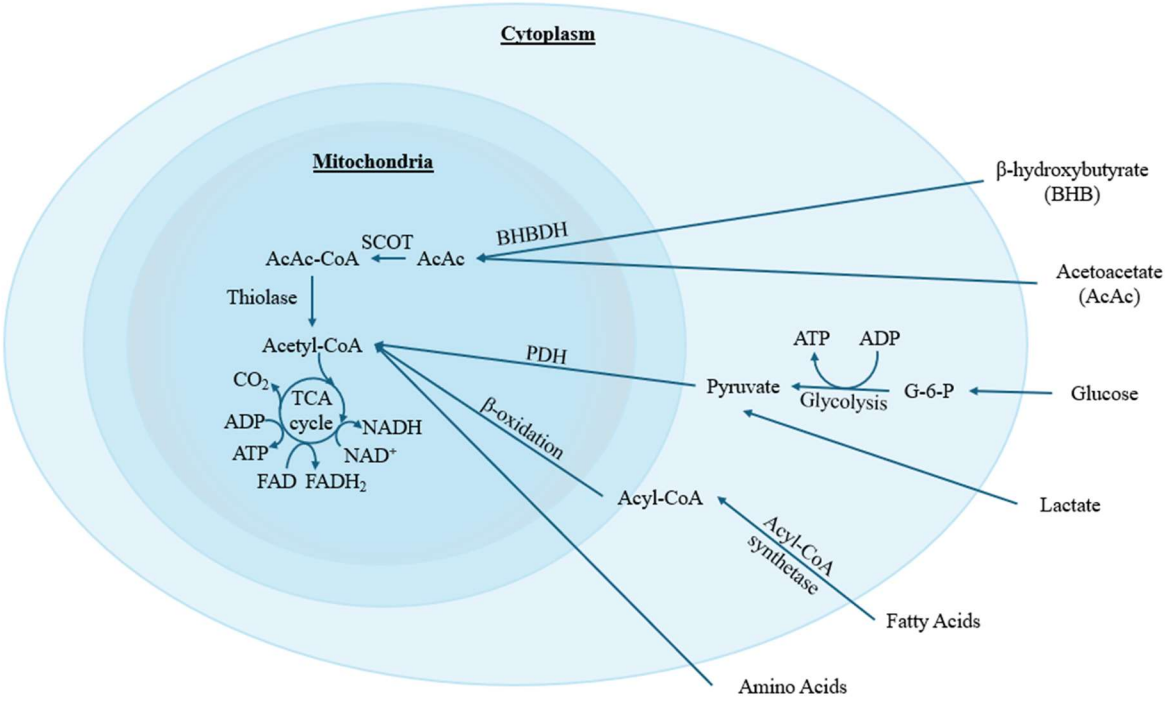

Figure 6: Various sources of energy for tissues.

Ketogenesis also occurs continuously in the hepatic mitochondria of a healthy person. But as mentioned earlier, under certain conditions such as an increased concentration of free fatty acids from adipose tissue or depleted carbohydrate reserves, the ketogenesis rate increases. As illustrated in Figure 7, fatty acids released from adipose tissue during lipolysis and derived from triacylglycerols (TAGs), are transported to the liver where they enter the mitochondrial matrix of hepatocytes through carnitine palmitoyl transferase 1 (CPT1). Three ketones are derived from the

β-oxidation of the excessive free fatty acids and the first substrate for ketogenesis is Acetyl-CoA. Here, the Acetyl-CoA can perform one of two tasks: 1) it can enter the TCA (Krebs) cycle as one of the intermediates to produce ATP and oxaloacetate which can undergo gluconeogenesis, and the glucose is exported as fuel for the brain and other tissues or 2) form acetoacetyl-CoA (AcAc-CoA) in a reaction catalyzed by thiolase. This acetoacetyl-CoA synthesizes 3-hydroxy-3-methylglutaryl-CoA (HMG-CoA) with the help of HMG-CoA synthase, which is further broken down into acetoacetate (AcAc) and acetyl-CoA (Ac-CoA) by the action of HMG-CoA lyase. This acetoacetate forms the other two ketone bodies, acetone by decarboxylation and D-3-hydroxybutyrate (BHB) by reduction [46].

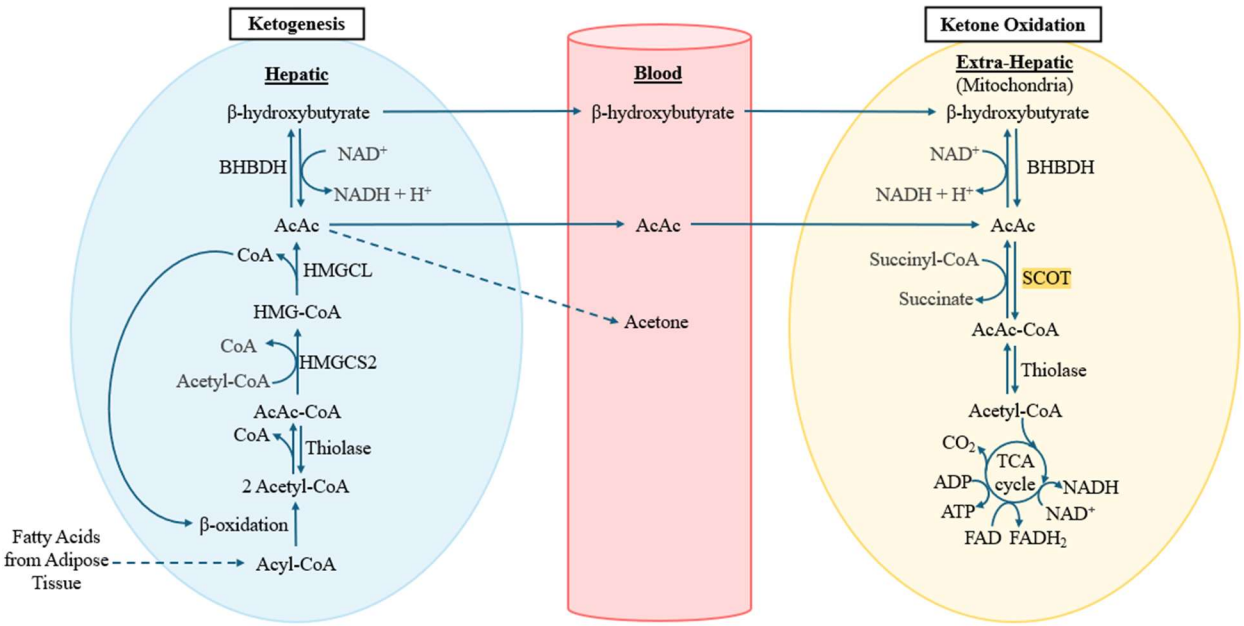

Figure 7: Ketogenesis and Ketone Oxidation

Since the liver does not have the enzyme β-keto-acyl-CoA transferase, it cannot use up the ketone bodies produced in the mitochondria and so AcAc and BHB are exported out of the liver and into the blood as sources of energy for the heart, skeletal muscles, and brain. Both these 4-C molecules can be converted back to Ac-CoA by most tissues of the body except the liver by ketone

oxidation. In the extrahepatic cells' mitochondria, BHB is converted back to AcAc by β-hydroxybutyrate dehydrogenase (HBD) with the release of NADH and H+. This AcAc is converted back to AcAc-CoA by β-keto-acyl-CoA transferase enzyme and this AcAc-CoA enters the citric acid cycle (TCA or Krebs cycle) and produces NADH, FADH2, ATP/GTP, and CO2 with each iteration of the cycle. The acetone that was produced by the decarboxylation of AcAc is exported out of the liver in the form of lactate which is then oxidized into pyruvate and ultimately converted to Ac-CoA, which fuels the TCA or Krebs cycle [44] [47].

These ketones must be expelled out of the body through the urine and usually, the process is fairly regular and pH dependent. But in cases of extreme form of ketosis or an out-of-control case of TIDM, there is ketoacidosis i.e., extremely elevated levels of KB in the blood, which makes the blood acidic. Diabetes mellitus is characterized by insulin deficiency and elevated glucagon levels, which can be maintained or regulated with periodic/controlled insulin replacement [48]. Normally, increasing glucose concentration leads to insulin production in pancreatic beta cells, and this insulin decreases blood sugar levels by inhibiting the gluconeogenesis and glycogenolysis processes. When such a T1DM patient is under high duress or stress (Figure 8), and/or fails to administer enough insulin, their blood sugar level drops, and blood ketone levels start to increase. They enter a pathological state of ketoacidosis with significantly low or absent levels of blood insulin which leads to increased gluconeogenesis and glycogenolysis, thus producing inappropriately elevated levels of glucose and plasma glucagon. This ultimately could lead to hyperglycemia [49].

Ketogenesis is also regulated by insulin and hormones such as glucagon, thyroid hormones, catecholamines, and cortisol increase the ketogenesis rate by stimulating the breakdown of free fatty acids. Due to the absence of carbohydrate reserves and no oxaloacetate left for condensation

with Ac-CoA, there is β-oxidation of fatty acids and ketone bodies are produced. As instructed, the liver produces exceedingly high concentrations of ketones, which lowers the pH of blood plasma to dangerous levels. This triggers the kidney to urinate with the urine being very highly acidic in nature. This urine is comprised of glucose and ketones that were not reabsorbed by the kidney due to the inability of the renal tubules, along with excessive water and many necessary electrolytes which leads to severe dehydration. Symptoms of ketoacidosis include frequent urination, breath smelling like fruits or acetone, nausea, shortness of breath, fatigue, and excessive thirst [50].

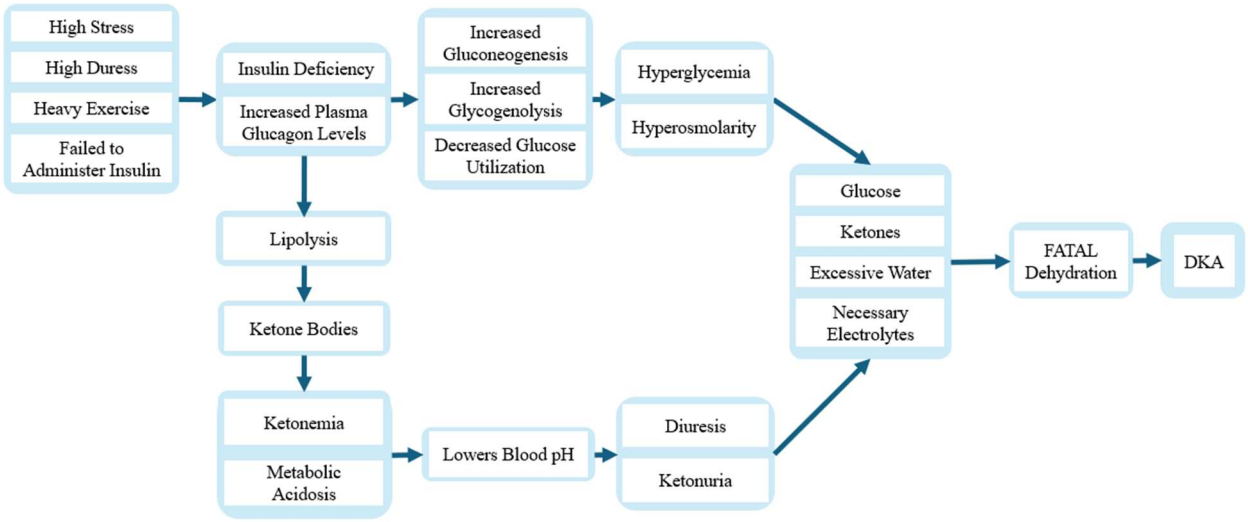

Figure 8: Risk of DKA in type 1 diabetes mellitus patients (T1DM)

The symptoms of diabetic ketoacidosis include hyperglycemia, dehydration, hyperosmolarity, osmotic diuresis, worsening renal functions, severe inflammation, and electrolyte imbalance. This is proof why understanding the critical role of ketogenesis in energy metabolism and the severe risks posed by DKA is extremely crucial, and why we need accurate and continuous monitoring of ketones. Here, traditional methods will often fall short, and this gap in effective monitoring calls for innovative solutions that can offer continuous, reliable, and minimally invasive measurement of ketone bodies.

2.3.2 Electrochemical HBD-based Biosensor for Enzymatic Detection

Biosensors, particularly microneedle technology, present a promising avenue for addressing this challenge. Biosensors are devices that convert biological or chemical information into electrical signals [51] [52]. As illustrated in Figure 9, a biosensor is comprised of two parts: the bioreceptor part and the transducer part. Biosensors can be classified into many types based on the bioreceptor type and the transducer component.

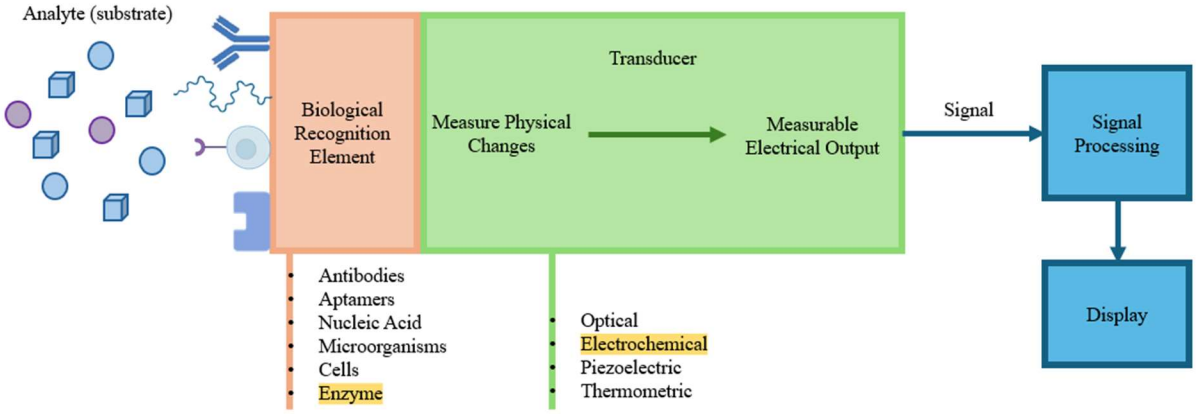

Figure 9: Schematic of Biosensors

Depending on the bioreceptor, biosensors can be classified into enzymatic, immunosensor, DNA sensor, and whole cell. Depending on the transducer, the biosensors can be categorized as electrochemical, optical, piezoelectric, thermal, and magnetic sensors. In this thesis, we use enzymatic biosensors, also known as biocatalytic sensors. These are biosensors that specifically utilize enzymes to catalyze a reaction with the target analyte. The enzyme's activity results in a measurable change, such as the production of a detectable electrochemical signal, which is used to quantify the analyte concentration.

Most studies to date have focused on dehydrogenase-based enzymatic biosensors, which are commonly used for decentralized testing of various analytes, such as alcohol and lactate. A dehydrogenase-catalyzed reaction is a biochemical process in which an enzyme known as a

dehydrogenase catalyzes the removal of hydrogen atoms (often in the form of protons and electrons) from a substrate. This reaction typically involves the oxidation of the substrate, where electrons (along with hydrogen ions) are transferred from the substrate to an electron acceptor molecule, such as NAD^+ (nicotinamide adenine dinucleotide) or FAD (flavin adenine dinucleotide). In a typical dehydrogenase-catalyzed reaction, the substrate ($A\text{-}H_2$) loses hydrogen atoms:

$$A{-}H_2 + NAD^+ \xrightarrow{A-Dehydrogen} A + NADH + H^+$$

Here, "$A\text{-}H_2$" represents the substrate with hydrogen atoms, and "A" is the oxidized product. NADH is the product of the selective dehydrogenase-catalyzed reaction with the target substrate. The detection mechanism of these biosensors involves the measurement of NADH which allows for the quantification of the substrate (illustrated in Figure 10).

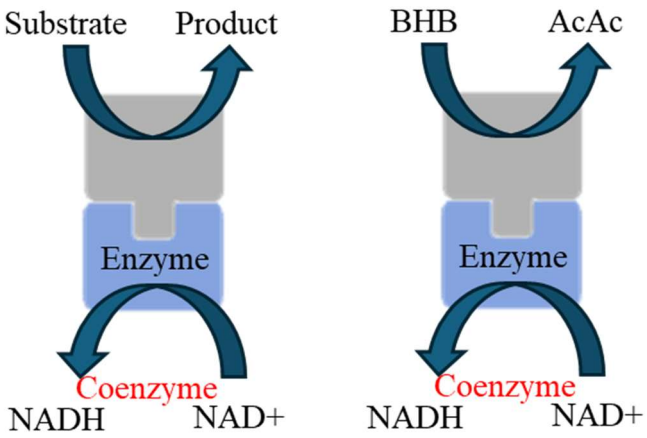

Figure 10: Dehydrogenase Enzyme Biocatalytic Reaction

For instance, in the case of the enzyme β-hydroxybutyrate dehydrogenase (HBD), the reaction involves the oxidation of β-hydroxybutyrate (BHB) to acetoacetate (AcAc), with NAD^+ reduced to NADH, which can then be measured:

$$BHB + NAD^+ \xrightarrow{BHB-Dehydrogenas} AcAc + NADH + H^+$$

Here we observe that NADH is a common biproduct of a dehydrogenase reaction. And the measurement of this NADH will allow for the quantification of the amount of substrate in the solution. Since our reaction produces a NADH molecule and we measure the NADH there is a need to use a redox mediator to reduce the oxidation potential of the NADH. This redox mediator would categorize this proposed solution into the 2nd generation of amperometric biosensors (Figure 11).

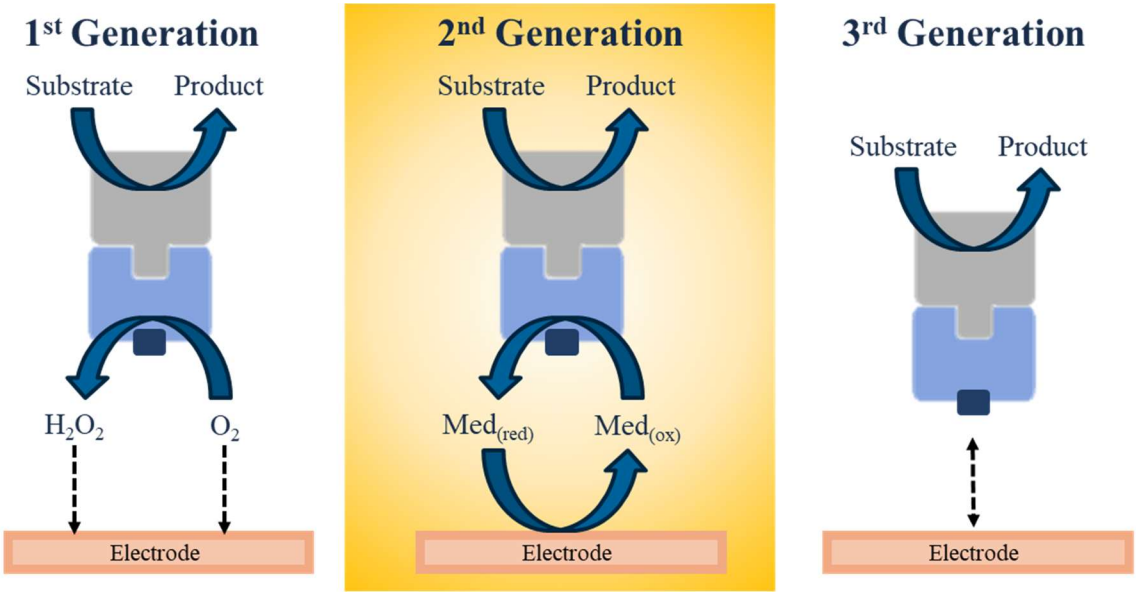

Figure 11: Generations of Ampermetric Enzymatic Biosensors

These reactions are foundational in the development of electrochemical biosensors for monitoring key metabolites, such as ketones, in medical diagnostics. The electrochemical sensor has an electrode that acts as a transducer, converting the biochemical reaction into an electrical signal. The electrode is typically made from materials like platinum, gold, carbon, or conductive polymers. The enzyme-catalyzed reaction typically produces or consumes electrons or generates products like NADH, which can be detected using electrochemical methods such as amperometry, voltammetry, or potentiometry. Electrochemical sensing devices are widely used due to their high

sensitivity, selectivity, cost-effectiveness, rapid response, convenience, potential for miniaturization, scalable manufacturing, and ease of integration into portable devices [53].

The solution we propose in this thesis is a dynamic biocatalytic detection mechanism for ketone detection, which has two steps: 1) selective reaction of BHB target metabolite with a NAD^+ cofactor-dependent HBD enzyme on the microneedle surface and 2) electrochemical transduction of the enzymatic reaction through amperometric detection of the NADH reaction product. These electrochemical sensors leverage the specific chemical properties of ketones and their interaction with enzymatic reactions, which generate electrical signals proportional to the concentration of ketones in the sample. The change in current (amperometric sensors) or voltage (potentiometric sensors) is measured and is proportional to the changes in concentration of the analyte (Figure 12).

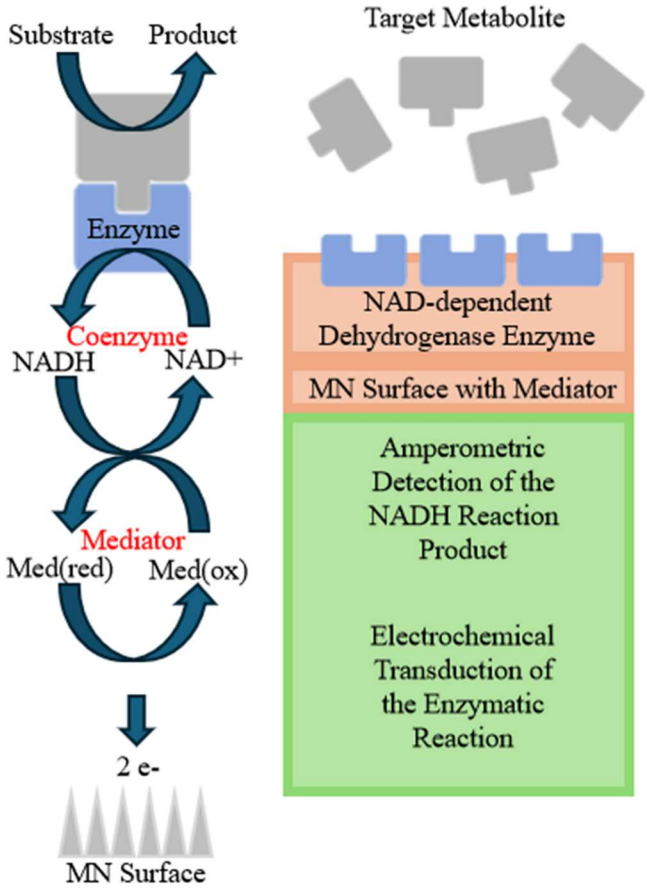

Figure 12: Actions of Enzymatic Electrochemical Biosensor

This new electrochemical biocatalytic microneedle biosensor for continuous BHB monitoring uses a NAD^+ cofactor dependent HBH enzyme. The NAD-dependent dehydrogenases are the largest group of redox enzymes known today and they don't have any oxidase-based enzyme limitations such as dependence on oxygen. However, they require the stable confinement (immobilization) of the NAD^+ cofactor on the microneedle surface. On top of that, the subsequent oxidation of NADH at the electrode surface commonly occurs at high potentials, which can lead to interference from other electroactive compounds like acetaminophen, ascorbic acid, or uric acid, as well as extreme surface fouling due to the adsorption of oxidized products, reducing the sensor's stability. Due to the challenges of stabilizing the NAD^+ cofactor and redox mediator, most HBD-based biosensors reported so far have been designed as single-use, disposable devices for self-testing. To mitigate these issues, redox mediators are employed to lower the oxidation potential of NADH.

$$BHB + NAD^+ \xrightarrow{BHB-Dehydrog} AcAc + NADH + H^+$$

$$NADH + Mediator_{(ox)} \rightarrow NAD^+ + Mediator_{(red)}$$

$$Mediator_{(red)} \rightarrow Mediator_{(ox)} + e^-$$

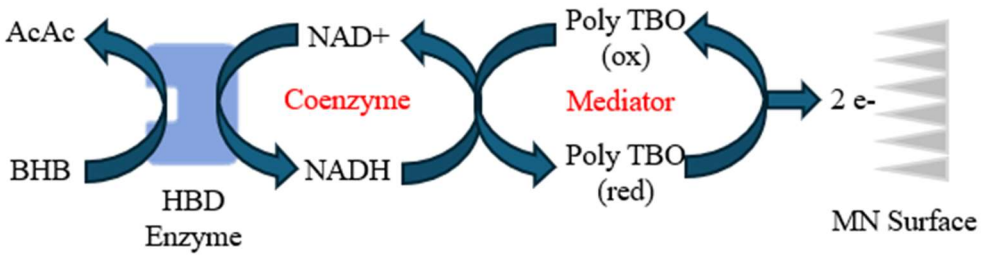

Figure 13: Actions of HBD Enzyme-based Electrochemical Biosensor

Hence, the detection of BHB is achieved through a coupled reaction mechanism that involves an enzyme, a cofactor, a mediator, and a transducing element (Figure 13). In this study, toluidine blue O (TBO) is used as the mediator, nicotinamide adenine dinucleotide (NAD^+) is used

as the coenzyme, and β-hydroxybutyrate dehydrogenase (HBD) is used as the enzyme, all of which are confined to the surface of the working electrode microneedle transducer (as seen in figure 13). The NADH produced by the NAD^+-dependent HBD-catalyzed reaction is then amperometrically detected at a low potential via the TBO-mediated reaction. This transition from metabolic processes to electrochemical detection underscores the seamless integration of biological knowledge with technological advancements, facilitating more accurate and timely monitoring of ketone levels in both experimental and remote settings. The BHB microneedle sensor goes another step further and offers a practical solution for tracking the physiological temporal profile of BHB in interstitial fluid (ISF) among individuals taking a ketone supplement.

Chapter 3 Methods and Materials

3.1 Chemicals

All the reagents and solvents for the preparation of the enzymatic microneedle patch sensor, in-vitro testing, and on-body monitoring, were used as received. For the enzymatic layers on the fabricated microneedle, chitosan (low molecular weight), glacial acetic acid (C2H4O2, ≥99.99%), gold (III) chloride trihydrate (HAuCl4.3H2O, ≥99.9%), hydrochloric acid (HCl, 37%), *β*-hydroxybutyrate dehydrogenase from *Pseudomonas lemoignei* (HBD, EC 1.1.1.30, 25 UN), *β*-nicotinamide adenine dinucleotide (reduced form, ≥97.0%), poly(vinyl chloride) (PVC), toluidine blue O (TBO, C15H16ClN3S, 94%), and Tris-HCl buffer solution (1 M, 7.5 pH) were purchased from Sigma-Aldrich. Carboxylated multiwalled carbon nanotubes (CNTs-COOH, >95%) were purchased from Cheap Tubes, Inc. Silver/silver chloride (Ag/AgCl) ink was obtained from Ercon, Inc.

Acetaminophen (C8H9O2N, ≥98.0%), L-ascorbic acid (C6H8O6, 99%), L-(+)-lactic acid (C3H6O3, ≥98%), and uric acid (C5H4N4O3, ≥99%) were purchased from Sigma-Aldrich and used for in-vitro testing of interference from co-existing electroactive species. D-(+)-glucose anhydrous (C6H12O6, ≥99.5%), sodium chloride (NaCl, ≥99%), and potassium chloride (KCl, ≥99.5%) from Sigma-Aldrich were used to prepare artificial/synthetic ISF based on the reported procedure [25] [54]. Phosphate buffer solution (1.0 M, pH 7.4) from Sigma-Aldrich was diluted to make PBS (0.1M, pH 7.4) solution. Stock solution for was prepared using *β*-nicotinamide adenine dinucleotide hydrate (oxidized form, ≥96.5%) from Sigma-Aldrich in PBS (0.1M, pH 7.4), and the stock solution for BHB was prepared using (+-)-sodium 3-hydroxybutyrate (C4H7O3Na, ≥99.0%) from Sigma-Aldrich, in both PBS (0.1M, pH 7.4) and artificial ISF.

3.2 Instrumentation and Sensor Fabrication

3.2.1 Electrochemical Analysis

All electrochemical measurements were conducted against Pt (bare) microneedles using a handheld, wireless potentiostat (Sensit BT, PalmSens) managed by PSTrace (PalmSens) software version 5.9. In vitro measurements of the NADH and BHB analytes were performed in PBS (0.1 M, pH 7.4) or in synthetic ISF using the respective stock solutions. On top of the testing surface modifications and microneedle modifications, a small 3D printed cylindrical tube (15 mm diameter and 15 mm height) of internal volume 1mL is embedded onto the MN patch surface. The sample solutions were placed in this 3D-printed, open-cylinder electrochemical cell to facilitate seamless testing and prevent leaks and leaching.

3.2.2 Fabrication of the Microneedle Patch Sensor

An array of 20 individual microneedles (10 working electrodes and 10 reference electrodes) is designed using SolidWorks and printed using Digital Light Processing (DLP) printing which employs a micro15 printer (Kudo3D). The microneedles are 1.5mm in height and 300μm in diameter with a microtip size of 20μm. The printed parts are cleaned in an isopropanol ultrasonic bath for 60 minutes, and UV-cured (405nm) for 30 minutes. The microneedles are outgassed in a vacuum oven at 80 °C overnight. To make handling of the microneedles easier, a base of 2.5cm diameter and a protective cover with holes for microneedle placements was designed in SolidWorks and printed using a Form3+ printer. The same post-printing processes are repeated for the printed parts (isopropanol ultrasonic bath for 60 minutes, UV cure at 50°C for 60 minutes, and outgassing the base in a vacuum oven) [55].

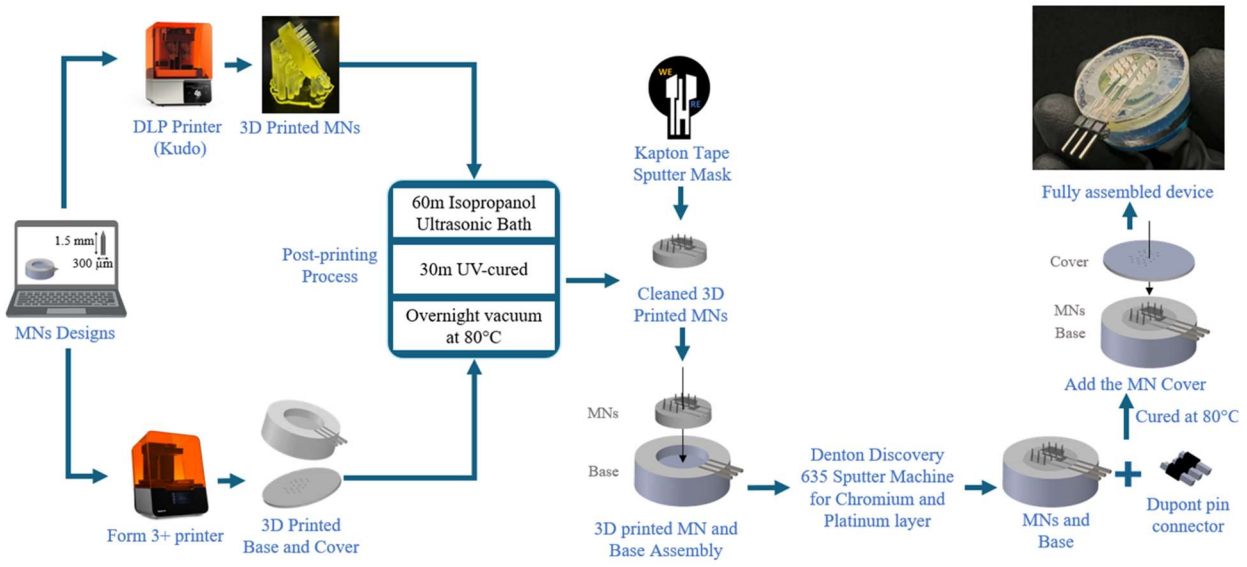

Figure 14: Fabrication and Assembly of MN Sensor

The microneedle is now assembled by attaching the microneedle array to the center of the printed base. A sputter mask is designed in Keynote and scored on Kapton tape using Cricut Explore Air 2. This is important to protect the two different sections of the microneedles from forming any connections, to differentiate distinctly between the working and the reference electrode, and to avoid short-circuiting. Then there is meta deposition on the microneedles using the Denton Discovery 635 machine of chromium layer (6 min at 300W) and platinum layer (12 min at 100W). Conductive silver epoxy and Dupont pin connectors are applied to the connection channels and cured at 80°C for 30 minutes. The 3D-printed cover is attached to the microneedle for protection and insulation by applying a thin layer of photocurable resin to the base and UV-curing the resin for 60 minutes (process summarized in Figure 14). After assembling, ensure the final height of the microneedles is 1.2 mm [55] [56].

3.2.3 Fabrication of the Enzymatic Microneedle Patch Sensor

The fabrication process of the enzymatic biosensor for BHB monitoring closely follows the ketogenesis process, the relation between AcAc and BHB, and the need to maintain the balance

of the NADH/NAD^+ (cellular redox state). Understanding the principles behind these is key to the development of a biocatalytic sensor that is highly selective, sensitive, and analyte-specific. The new CKM microneedle patch sensor leverages a gold-electrodeposited platinum transducer. A 100μL of a 1.0 mM Gold (III) chloride solution dissolved in 0.1 M HCl is used to electrodeposit an initial gold (Au) layer onto the Pt working electrode of the microneedles (WE) by applying a potential of -0.9 V for 20 min. This is done to improve the signal strength of the WE. After 20 min the electrode surface is rinsed with PBS buffer and air-dried at room temperature.

For testing the electrochemical response of the sensor for NADH, which generally happens at higher oxidation potentials, there is a need to lower the oxidation potential using a redox mediator. So, following the Au electrodeposition, this transducer is enhanced with an electropolymerized layer of toluidine blue O (poly-TBO), which serves as a mediator. 1μL droplet of a 0.2 mM TBO solution (redox mediator) is cast onto the MNs and allowed to dry for 45 min. The TBO film is then altered through electropolymerization, utilizing a disposable Ag/AgCl pseudo-reference electrode strip in a two-electrode system. A 0.9V potential is applied for 6 minutes with 400μL of PBS solution (0.1 M, pH 7.4), followed by multiple rinses with deionized (DI) water to form poly-TBO. This modified poly-TBO/Au/Pt MN patch is used to evaluate NADH detection.

Now for the evaluation of BHB detection, we need to recreate the seamless conversion of BHB to AcAc with the help of HBD enzyme, and the release of the NADH product. However, the HBD enzyme is a NAD^+ dependent enzyme and the NAD^+ coenzyme requires stable confinement (immobilization) on the surface of the MNs. To achieve this, the next layer consists of a biocatalytic coating made up of the β-hydroxybutyrate dehydrogenase (HBD) enzyme and the nicotinamide adenine dinucleotide (NAD^+) coenzyme. 1μL of a cocktail solution of carboxylated

CNTs (0.1 mg mL^{-1}) in chitosan solution (0.5 wt. % in 0.1 M acetic acid) is placed on each of the modified WEs of the MN patch and allowed to air-dry at room temperature. This is followed by the deposition of 1µL of a mixture of HBD (2.5 mg mL^{-1}) in 0.1 M Tris-HCl buffer solution, NAD^+ (40.0 mM) in 0.1 M Tris-HCl buffer (1:2 v/v ratio), and chitosan (0.5 wt. % in 0.1 M acetic acid) on the modified WEs of the MN patch and facilitating overnight incubation at 4°C.

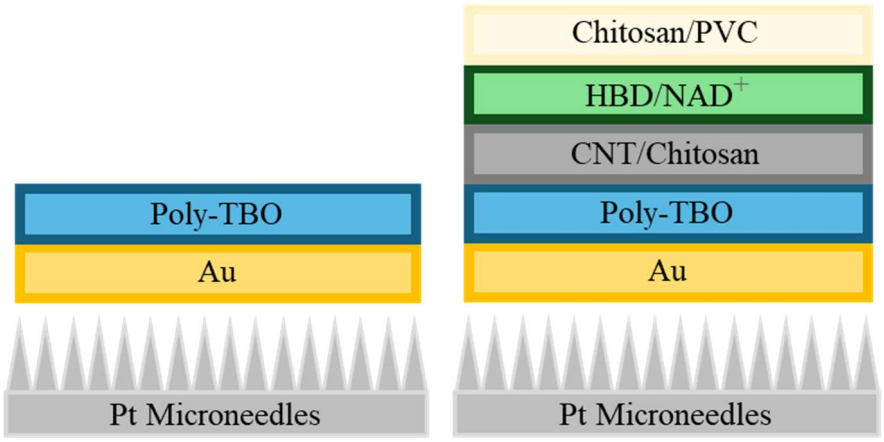

Figure 15: Enzymatic Modifications of Electrochemical MN Biosensor

Additionally, chitosan (Chit) and poly(vinyl chloride) (PVC) are applied as protective layers to enhance stability and selectivity. 1µL of 0.5% chitosan solution and 1µL of 2.0% poly(vinyl chloride) (PVC) solution are added on the surface and they are stored at 4°C until used. All the layers indicated in Figure 15. Here, CNTs/chitosan assist in immobilizing HBD and NAD^+ through amide bonds whereas, chitosan is utilized in two steps during sensor development to ensure strong immobilization of HBD/NAD^+ biomolecules through covalent bonds. The wearable microneedle-based sensor device is thus designed with a Pt working electrode that incorporates the HBD enzyme, paired with a quasi-reference Pt electrode, providing an effective platform for in vivo BHB monitoring as summarized in Figure 15.

3.3 Procedure

3.3.1 In Vitro Evaluation of Ketone using Microneedle Sensor

After fabricating microneedle patch sensors and before starting the in-vitro experimentations, it is essential to perform a critical step in modifications in the development of the biosensors based on dehydrogenases which is to select an appropriate electrocatalytic mediator [57]. This mediator should be able to effectively reduce the potential for NADH oxidation to the desired level which is critical to avoid any interference from other oxidizable components in interstitial fluid (ISF), as well as achieve low background current and noise. Furthermore, the mediator must have a high electron transfer rate and a highly selective biocatalytic reaction with NADH in order to efficiently regenerate NAD^+ as the final product [58] [59]. This was achieved by comparing multiple potential redox mediators and critically evaluating their surface functionalization for selective and stable NADH measurements. Many different redox mediators were screened for NADH detection by recording chronoamperograms of Au/Pt SPCE electrodes, each modified with a different redox mediator: azure C (AC), meldola blue (MeB), methylene blue (MB), methylene green (MG), nile blue A (NBA), phenanthroline dione (PD) and toluidine blue O (TBO) in PBS media (0.1 M, pH 7.4) spiked with 5mM NADH. The corresponding current readings were saved and plotted.

Poly-TBO was chosen as the redox mediator and the redox mediator-modified poly-TBO/Au/Pt microneedle patch sensor is ready for use. Now, there is a need to validate whether the poly-TBO/Au/Pt MNs are better at in-vitro NADH measurements when compared to Au/Pt and bare Pt MNs. These three MNs patch sensors were subjected to low potential NADH catalysis using cyclic voltammetry, with a scan rate of 0.05 V/s and a scan range of -0.4 V to +0.5 V, in PBS (0.1 M, pH 7.4) before and after the addition of 2mM NADH and the corresponding CVs

were recorded. Post that, the bare Pt MNs sensor and the poly-TBO/Au/Pt MNs sensors were compared using chronoamperometry in PBS (0.1 M, pH 7.4) before and after the addition of 1mM NADH at various applied potentials ranging from 0-0.4 V.

Now after determining the optimum NADH oxidation potential, the same potential is used to assess the sensitivity, selectivity, stability, reproducibility, and shelf life of the poly-TBO/Au/Pt MNs sensors one by one. For sensitivity, the limit of detection (LOD) must be determined by creating a standard curve and a calibration plot which would serve as the baseline for all future experimentations. Chronoamperometry is performed on the modified poly-TBO MN sensor at the optimum applied potential of +0.2 V by successive additions of 0.05 mM concentrations of NADH until it reaches up to 1.5mM (1 to xxx). The resulting current responses are recorded and plotted, and a calibration plot is made by taking the value of the current response at the 60s mark for each concentration.

To assess the selectivity of the poly-TBO/Au/Pt MNs sensor at the optimum NADH detection potential and get corresponding current responses, chronoamperometry was performed for 1mM NADH detection in the presence of common interferents: 6.25µM acetaminophen (AP), 5µM ascorbic acid (AA), 5mM glucose (Glu), 1mM lactate (Lac), and 150µM uric acid (UA). The resulting chronoamperometric current responses and relative current responses were plotted.

To assess the operational stability of the poly-TBO/Au/Pt MNs sensor at the optimum NADH detection potential, the sensor underwent repetitive chronoamperometric measurements of 1mM NADH concentrations at room temperature at 15 min intervals for a period of 5 h. Another test performed was taking amperometric response of the poly-TBO/Au/Pt MNs sensors over extended periods while making successive additions of NADH in low concentrations a) 0.05mM

and high concentrations b) 0.25mM amounts. The resulting data was recorded and plotted along with the subsequent calibration plot.

This is followed by tests for reproducibility and shelf-life storage. For both these assessments, chronoamperometry was performed at 1mM NADH concentrations. In reproducibility assessment, 5 poly-TBO/Au/Pt MNs sensors are tested under the same condition and the results are plotted. For the shelf-life assessment, the poly-TBO/Au/Pt MNs sensor is tested over a 15-day period repeatedly, during which the sensor is stored at room temperature each time until use.

These studies assess whether the mediator-based poly-TBO/Au/Pt microneedle (MN) sensor meets the necessary criteria for effective NADH detection or not. At this point, modifications are made to the poly-TBO/Au/Pt MN sensor to convert it into an enzymatic biosensor which is crucial for the subsequent operation of a selective, sensitive, and stable continuous ketone monitoring (CKM) system based on β-hydroxybutyrate (HBD).

Much like the assessments of NADH concentrations by the poly-TBO/Au/Pt MNs sensors, the BHB detection of the modified biosensors also follows a similar assessment structure but, in both PBS, (0.1M, pH 7.4) and artificial ISF. After incorporating the NAD-dependent HBD biocatalytic layer in combination with chit and PVC, the assessments are carried out for the detection of the BHB target by first confirming the inability of the poly-TBO/Au/Pt MNs sensors without the immobilization of HBD/NAD^+ biomaterials to detect BHB. This is done by taking chronoamperometric measurements before and after the additions of 2mM BHB. The resulting chronoamperometric response is recorded. For comparison, it is important to successfully validate the BHB target analyte being catalyzed in the presence of HBD/NAD^+ by using CV and recording the modified MN sensor in PBS (0.1 M, pH 7.4) before and after the addition of 2 mM BHB. Now

the next step is to validate if the pH of the artificial ISF is a variable in the subsequent BHB detections. To do that, the chronoamperometric response of the BHB MN sensors is taken before and after the addition of 2 mM BHB under different pH of synthetic ISF (6.5pH, 7pH, 7.4pH, 8pH) along with the comparison of current responses.

Like the in-vitro assessment of NADH detection of the poly-TBO/Au/Pt MNs sensor, we determine the optimum BHB oxidation potential and use the same potential to assess the sensitivity, selectivity, stability, reproducibility, and shelf life of the HDB/NAD^+ modified MN sensors. For sensitivity, the limit of detection (LOD) must be determined by creating a standard curve and a calibration plot which would serve as the baseline for all future experimentations. Chronoamperometry is performed on the modified enzymatic sensor at the optimum applied potential of +0.2 V by successive additions of 0.5mM concentrations of BHB until it reaches up to 5mM (1 to xxx) in PBS. The resulting current responses are recorded and plotted, and a calibration plot is made by taking the value of the current response at the 60s mark for each concentration. This process is repeated with all the same conditions for BHB detection in artificial ISF.

To assess the selectivity of the HDB/NAD^+ modified MN sensor at the optimum BHB detection potential and get corresponding current responses, chronoamperometry was performed for 2mM BHB concentration in the presence of common electroactive interferents: 6.25µM acetaminophen (AP), 5µM ascorbic acid (AA), 5mM glucose (Glu), 1mM lactate (Lac), and 150µM uric acid (UA). The resulting chronoamperometric current responses and relative current responses were plotted.

To assess the operational stability of the HDB/NAD^+ modified MNs sensor at the optimum BHB detection potential, the sensor underwent repetitive chronoamperometric measurements of

2mM BHB concentrations at room temperature at 15 min intervals for a period of 5 h. Another test performed was taking the amperometric response of the HDB/NAD^+ modified MN sensors over extended periods while making successive additions of 0.5 mM BHB in artificial ISF, extending to 5mM. The resulting data was recorded and plotted along with the subsequent calibration plot. The stability of the microneedle biosensor is also assessed through continuous 5 h measurements of 0.2 mM BHB. And the resulting current response is recorded.

This is followed by tests for reproducibility and shelf-life storage. For both these assessments, chronoamperometry was performed at 1mM BHB concentrations. In reproducibility assessment, 5 HDB/NAD^+ modified MN sensors are tested under the same condition and the results are plotted. For the shelf-life assessment, the HDB/NAD^+ modified sensor is tested over 15 days repeatedly at room temperature, during which the sensor is stored at 4°C each time until use.

3.3.2 On-Body Test of Ketone using Microneedle Sensor

It's important to note that the thickness of human skin varies across different parts of the body. The outermost layer of the epidermis typically measures between 0.1 and 0.3 mm, while the underlying dermis layer can range from 0.5 to 3 mm in thickness. Microneedles (MNs) are designed to penetrate the outer skin layer and remain within the epidermis, which enables real-time measurement of analytes like BHB. These microneedles are capable of reaching the ISF at depths of less than 1 mm, where such measurements can be effectively taken. In our design, each microneedle in the array has a height of 1.2 mm, offering a sensing surface area of 0.92 mm^2, which is optimal for accurate and reliable sensing of BHB levels in real time. Post in-vitro experimentations, the cytotoxicity and skin penetration of the developed enzymatic ketone microneedle sensors are assessed to ensure the sensor would not cause any harmful effects from

direct skin contact, skin penetration, potential leaching of materials in or on the skin, or detachment of the sensing component.

THP-1 cells were cultured at a concentration of 1 × 10^6 cells/mL in RPMI medium. The THP-1 cells are a human monocytic cell line derived from an acute monocytic leukemia patient. These cells are widely used in biomedical research, particularly in studies related to the immune system, inflammation, and various disease processes. Due to their human origin and characteristics, THP-1 cells serve as a relevant in-vitro model for investigating the behavior of monocytes and macrophages, and they are commonly used in cytotoxicity assays.

The sensors were sterilized with UVC radiation and then incubated with the cell culture for two different periods: 1 hour and 24 hours. After incubation, 50μL of the MTS assay reagent (Colorimetric, ab197010) was added to each tube containing 500μL of the THP-1 cell (1 × 10^6 cells/mL) solution. The MTS assay is a colorimetric method used to assess cell viability, where the level of cytotoxicity is indicated by the reduction of MTS (tetrazolium salt) to a formazan product by metabolically active cells. This reduction occurs only in metabolically active cells, so the amount of formazan produced correlates with the number of viable cells. After a 40-minute incubation at 37 °C, the results were measured using UV spectroscopy at a wavelength of 490nm (as the formazan product is usually colored purple or blue and often measured at wavelengths like 490nm) with the BioTek Synergy Mx microplate reader. The intensity of the color is directly proportional to the number of living cells in the sample and in cytotoxicity assays, a decrease in formazan production compared to the control indicates the extent of cell death or reduced metabolic activity. This is often used to assess the toxicity of substances or the efficacy of treatments. This process allowed the researchers to determine the cytotoxic effects of the microneedle sensors on the cells, providing important data on the biocompatibility of the sensors.

In this test, the MN sensor sample in incubation was categorized into three instances: control, before skin penetration, and after skin penetration. The resulting data was plotted in terms of relative cell viability. Since this test deals with before and after skin penetrations, it is important to discuss on-body in-vivo human trials procedure and the assessments.

Healthy and consenting participants between the ages of 18-45 with no history of medical conditions like diabetes, gout, hyperuricemia, chronic kidney disease, GI symptoms, or renal/genitourinary abnormalities were selected for the trial. The trials were conducted under strict adherence to the ethical guidelines and protocol approved by the Institutional Review Board at the University of California, San Diego (IRB# 171927). For the trials, sterilized modified microneedle sensor patches were applied to the forearms of the participants, either on the left or right hand, using double-sided 3M medical adhesive tape to ensure secure placement (Figure 16A, 16D). Additional medical tape was placed over the MN sensor to further support the patches and prevent them from detaching. The microneedle sensor patches were then connected to the Sensit BT device using male-to-female jumper Dupont wires. The female end of each wire was attached to the male header pins on the sensor patch, while the male end was connected to the adapter on the Sensit BT, as illustrated in Figure 16A.

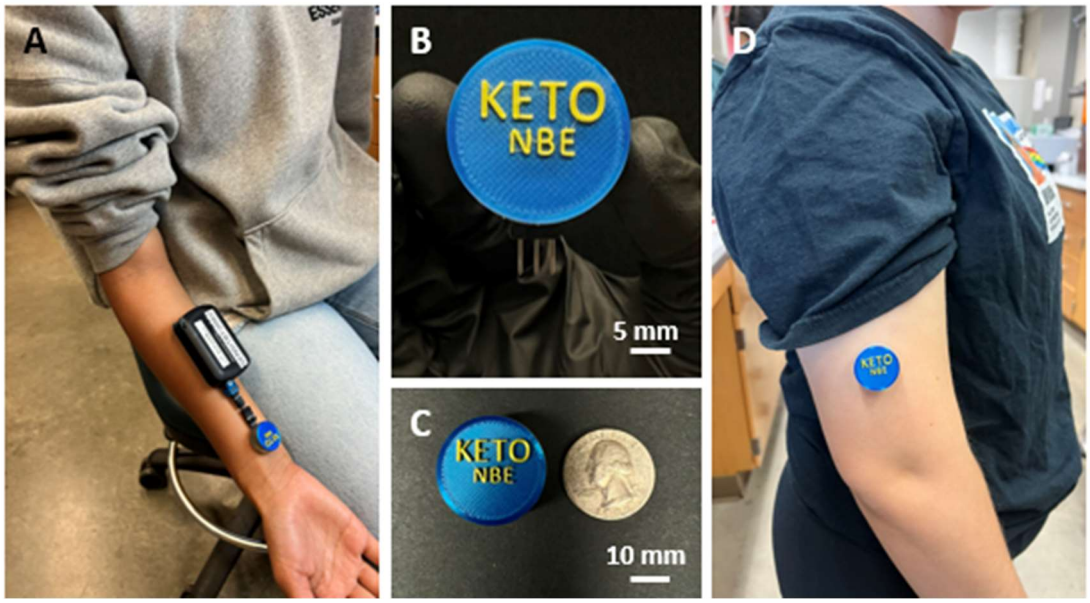

Figure 16: Microneedle Sensor On-body Placement

After checking all the connections and securing the placement of the microneedle, the trials start by applying a potential of +0.2 V to the sensor and waiting until a stable baseline current is established. Throughout the experiments, continuous fixed-potential amperometric detection is performed by the Sensit BT device and it is used to monitor changes in ketone levels based on the response from the MN sensor. The response of the sensor to ketone levels is cross-verified every 10 minutes using a commercial blood ketone meter (Keto-Mojo ketone analyzer) to ensure accuracy and validity. Once a stable baseline current is established, which typically occurs within the first 120 minutes, the participants are instructed to consume a commercial ketone drink (Real Ketones) containing 13.1 grams of ketone salts. The microneedle sensor continues to monitor the ketone levels in real-time, in the background, as the drink gets metabolized.

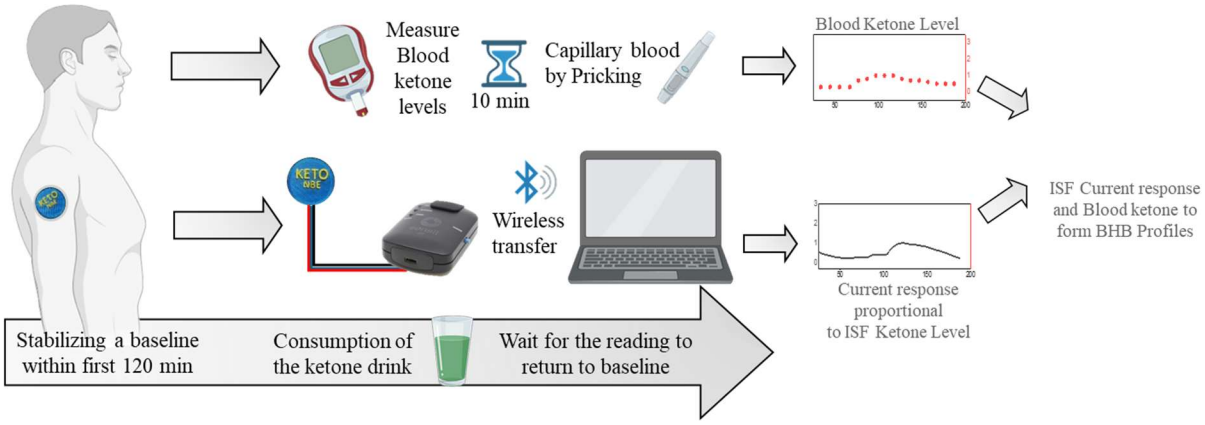

Figure 17: On-Body Testing Procedure

After the trials, the data from the sensor is transferred to a laptop or smartphone wirelessly, and retrospectively calibrated using two key reference points: the baseline current and the peak maximum current recorded during the trial. These calibrations allow the researchers to establish personalized ISF BHB profiles for each participant, by comparing the recorded current responses to the corresponding blood BHB concentrations. This process (illustrated in Figure 17) ensured that the sensor's readings were accurately aligned with the participant's actual ketone levels, providing reliable data on the effectiveness of the microneedle sensing system.

In this thesis, Chapter 3 is based, in part, on the material as it appears in journal of ACS Sensors, 2024, by Chochanon Moonla, Maria Reynoso, Ana Casanova, An-Yi Chang, Omeed Djassemi, Aishwarya Balaje, Amal Abbas, Zhengxing Li, Kuldeep Mahato, and Joseph Wang. The dissertation author was a co-author of this paper.

4.1 Screening Redox Mediator

As seen from Figure 18, the chronoamperometric assessment along with the corresponding current responses, the polymeric form of methylene blue (MB) initially showed a stronger signal than toluidine blue O (TBO), closely followed by nile blue A, but there was a change in the solution's color for MB which indicated that it had leached into the surrounding medium. This leaching most probably happened due to the presence of incomplete or deformed polymeric methylene blue residues that remained on the sensing surface along with properly polymerized form even after electropolymerization. This didn't occur in the case of electropolymerization of TBO, as it left no free-form TBO behind. The polymerized poly-MB also appeared to have higher solubility than poly-TBO under the same preparation conditions. Consequently, electropolymerized TBO was chosen for the development of the BHB microneedle sensing system as the polymerized form of TBO effectively reduces the risk of leaching from the sensing surface while maintaining its desirable redox mediator properties.

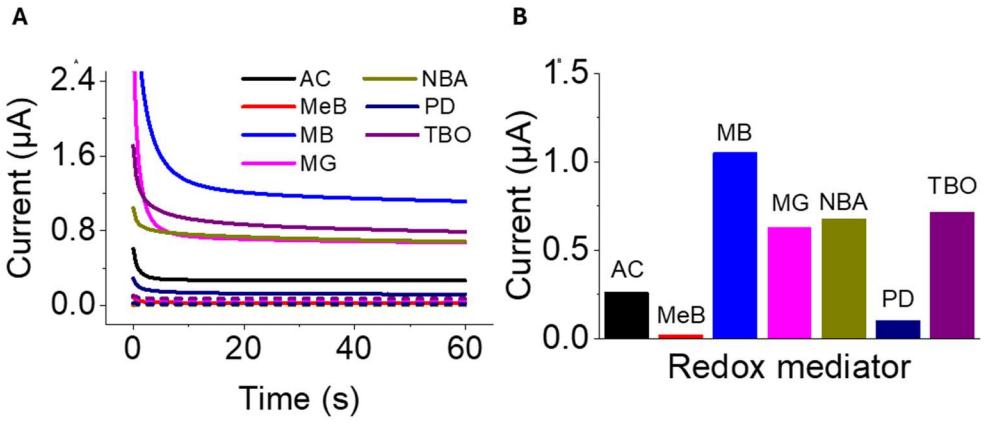

Figure 18: Screening Redox Mediators

4.2 In-vitro NADH Measurement using Microneedle Sensor

As seen from the CV Figures 19A-C, there is a clear trend of a shift in the NADH oxidation potential from bare Pt MNs to poly-TBO/Au/Pt MNs sensor. A NADH oxidation potential of around +0.4 V which is lower in Au/Pt at slightly above +0.3 V. This is significant but the most notable is the change in the NADH oxidation reaction to a much lower potential in the MNs sensors with poly-TBO redox mediator. With the combined efforts of electrodeposited Au and the poly-TBO on the surface, the sensors have higher sensitivity and show improved detection of NADH.

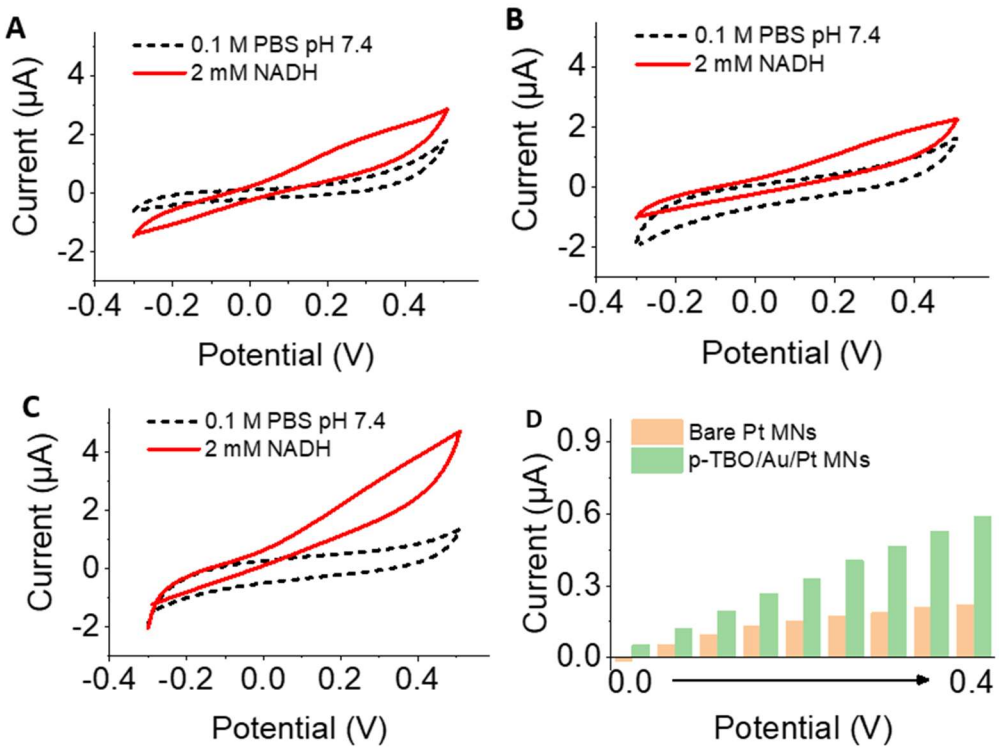

Figure 19: CV response of A) Pt vs B) Au/Pt vs C) poly-TBO/Au/Pt MN sensor in PBS (0.1M, pH 7.4) before and after the addition of 2mM NADH spike against Pt RE with scan rate 0.05 V/s and corresponding CV data for Pt vs poly-TBO/Au/Pt MN sensor for the range of 0-0.4 V

Based on the recorded CV for the range of 0-0.4 V (Figure 19D), chronoamperometry investigations for the same range were performed in PBS (0.1M, pH 7.4) before and after the addition of 0.1 M NADH in bare Pt and poly-TBO/Au/Pt MNs. From Figure 20, it is clearly

observed that the modified MNs showed higher response and sensitivity to NADH spiking at the same potential. One limitation that was observed was that although for higher detection potentials of +0.4 V, higher sensitivity was observed but there was a compromise to the selectivity. There was a rise in background currents, noise, and interference from electroactive constituents. Between 0-0.4 V, a detection potential of +0.2 V offered a balance between high sensitivity and selectivity allowing us to detect NADH from a range of 0.05mM to 1.5mM concentrations.

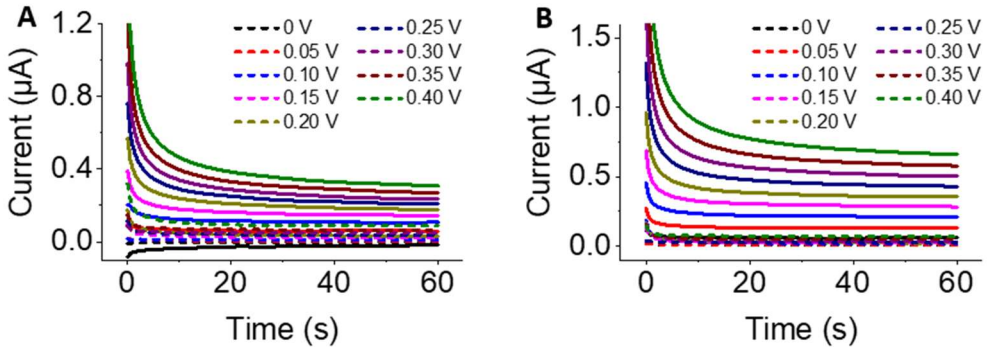

Figure 20: Chronoamperometry investigations for the range of 0-0.4 V in PBS (0.1M, pH 7.4) before and after the addition of 0.1 M NADH in A) bare Pt and B) poly-TBO/Au/Pt MNs.

The resulting chronoamperogram (Figure 21A) showed increasing current response for all 30 readings ranging from 0.05mM to 1.5mM at applied detection potential of +0.2 V. The resulting calibration plot (Figure 21B) shows a linear relationship with $R^2 = 0.951$. Based on the current responses in the chronoamperograms, the limit of detection (LOD) was assessed as 0.021mM NADH using the 3Sd/m criteria, where Sd is the standard deviation of the background signal for 0.05mM NADH, and the m is the slope of the calibration plot.

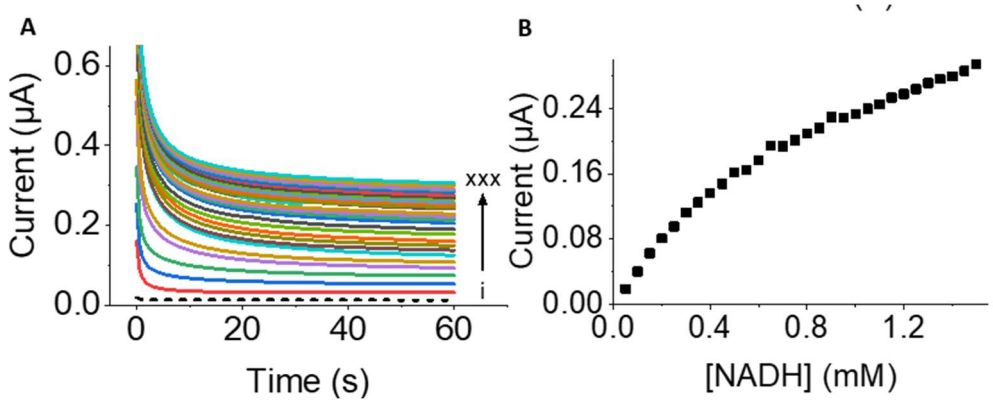

Figure 21: Sensitivity validation using A) Chronoamperogram at applied detection potential of +0.2V ranging from 0.05mM to 1.5mM and B) its corresponding calibration plot

The resulting chronoamperometric current response from selectivity analysis (Figure 22) and the corresponding relative current response indicated that the potential interferents are negligible compared to the target NADH detection and that the MN sensor are selective only for the target analyte and not the common interferences.

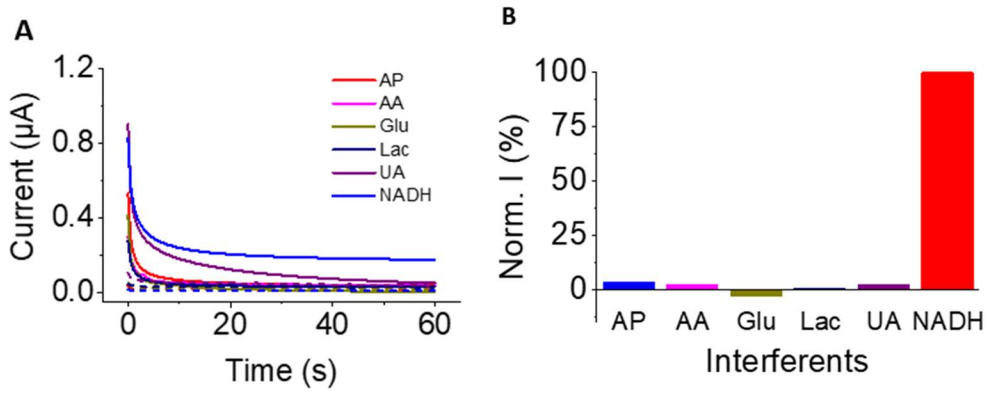

Figure 22: Selectivity analysis using A) Chronoamperometric current response of potential interferents and NADH, and B) its corresponding relative current response

The resulting curve (Figure 23A) shows 24 repetitive measurements of 1mM NADH concentration at the detection potential of +0.2 V. This data was used to plot a relative current response graph over the 5 h of repetitive testing to show that there is a high stability with a retention of 95% of the initial current response, and no compromise in the stability of the sensor over

extended period of operation (Figure 23B). This is the most critical aspect needed to support on-body testing capabilities.

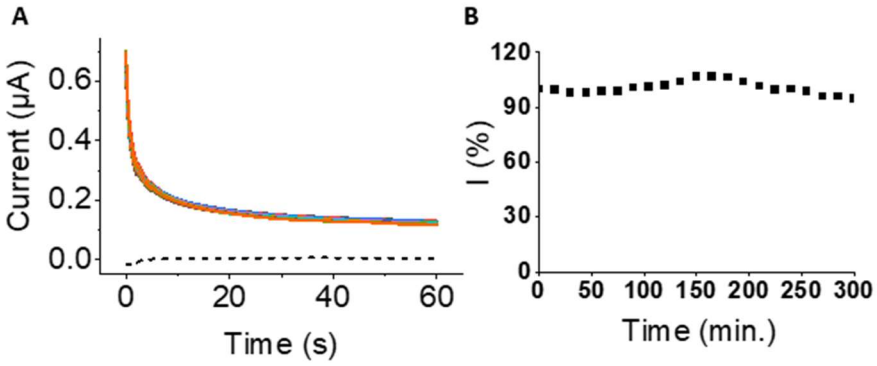

Figure 23: Stability analysis via A) chronoamperogram of repeated 24 measurements of 1mM NADH at +0.2 V and B) its corresponding relative current response plot

The resulting amperometric plots from the successive addition of NADH in low concentrations (0.05mM – 0.5mM) (Figure 24) and high concentrations (0.25mM-1.25mM) and the corresponding calibration plot show that there is a well-defined response and linear trend with similar sensitivity, respectively. [3]

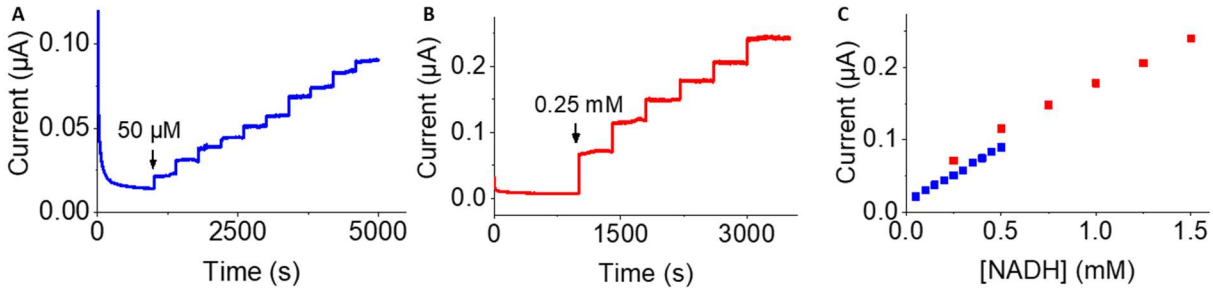

Figure 24: Sensitivity and stability analysis via A) amperometric plots with successive additions of A) low concentration 0.05mM and B) high concentration 0.25mM, and C) their corresponding calibration plot

The resulting chronoamperogram (Figure 25A) and the relative current response plot (Figure 25B) for the 5 poly-TBO/Au/Pt MNs sensor for reproducibility clearly indicate a very high reproducibility, with a relative standard deviation (RSD) of 1.39%.

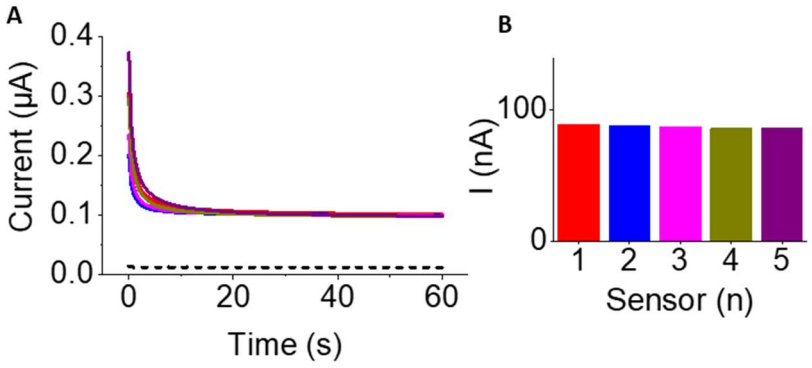

Figure 25: Reproducibility analysis via A) chronoamperometric detection of 1mM NADH in 5 poly-TBO/Au/Pt MN sensors under same conditions and B) the relative current response

The resulting chronoamperogram (Figure 26A) and the relative current response plot (Figure 26B) over the 15-day period for shelf-life/storage indicate a good shelf-life with an RSD of 1.82%. The sensor's performance in NADH detection ensures that it can reliably support the specific and sustained monitoring required for accurate ketone measurement.

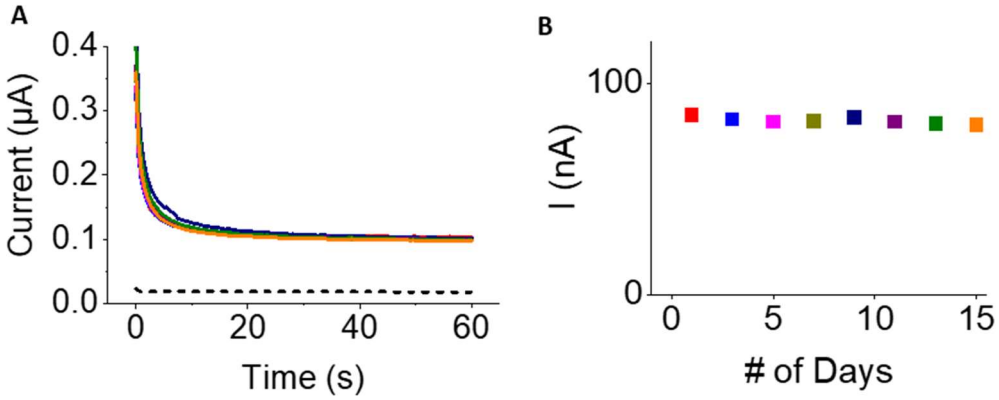

Figure 26: Shelf-life validation of modified MN sensors via A) chronoamperometric detection of 1mM NADH over different shelf-life periods and B) the relative current response plot

4.3 In-vitro BHB Measurement using MN Sensor

As anticipated, when BHB is introduced to the poly-TBO/Au/Pt MNs sensors with no immobilized HBD/NAD^+ biomaterials, there is no detectable response in the system (Figure 27A). This lack of response confirms that the presence of these specific biomaterials is essential for the sensor's functionality. The immobilization of HBD and NAD^+ is crucial because these components enable the biochemical reaction necessary for detecting BHB. Without them, the sensor remains inactive, as there is no BHB to NADH conversion and if there is no NADH, there is no electron transfer. The CV successfully validated the catalysis of BHB target in the presence of HBD/NAD^+ in PBS (0.1 M, pH 7.4) before and after addition of 2 mM BHB (Figure 27B).

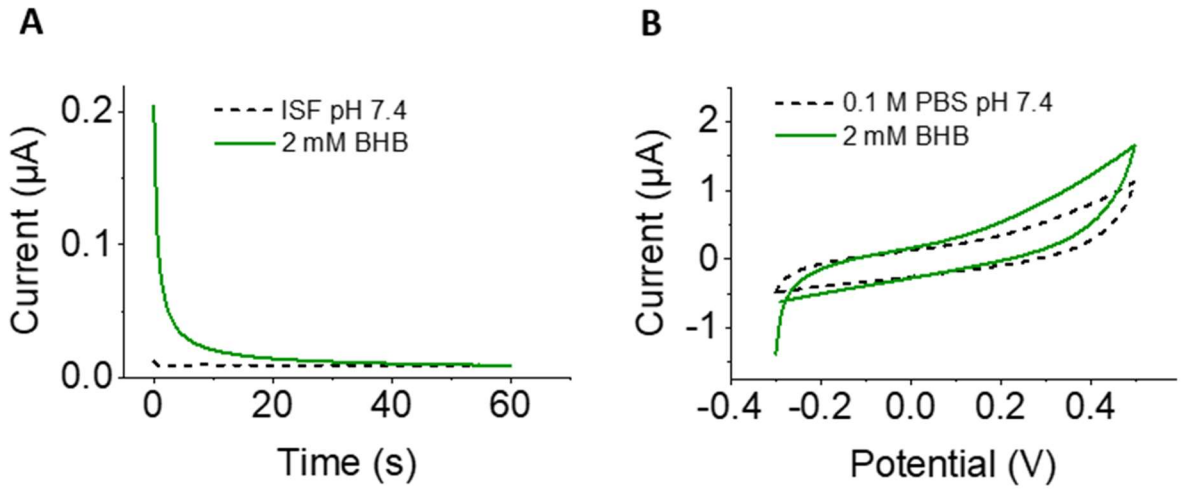

Figure 27: A) Chronoamperogram of 2mM BHB in poly-TBO/Au/Pt sensor without enzyme immobilization and B) CV validation of catalysis of 2mM BHB in the presence of HBD/NAD^+

The resulting chronoamperogram for BHB detection in PBS showed increasing current response for all 10 readings ranging from 0.5mM to 5mM in PBS (Figure 28A). The resulting calibration plot (Figure 28B) shows a linear relationship with R2 = 0.993 in PBS. Based on the current responses in the chronoamperograms, the limit of detection (LOD) was assessed as

0.05mM BHB in PBS using the 3Sd/m criteria, where Sd is the standard deviation of the background signal for 0.5mM NADH, and the m is the slope of the calibration plot.

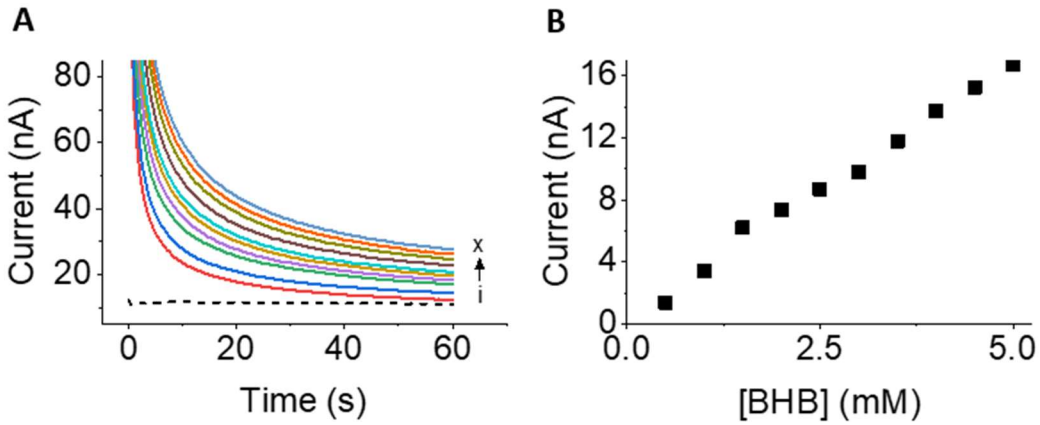

Figure 28: Sensitivity analysis in PBS via A) Chronoamperometric detection of 2mM BHB with successive increment of 0.05mM and B) the corresponding calibration plot

Similarly, the resulting chronoamperogram for detection in ISF showed increasing current response for all 10 readings ranging from 0.5mM to 5mM in ISF (Figure 29A). The resulting calibration plot (Figure 29B) shows a linear relationship with R2 = 0.999 in ISF. Based on the current responses in the chronoamperograms, the limit of detection (LOD) was assessed as 0.053mM BHB in ISF using the 3Sd/m criteria.

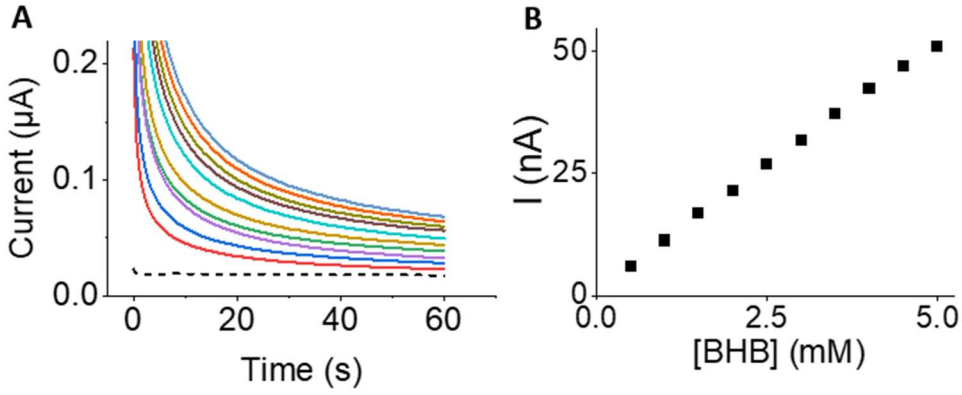

Figure 29: Sensitivity analysis in ISF via A) Chronoamperometric detection of 2mM BHB with successive increment of 0.05mM and B) the corresponding calibration plot

The modified MN sensor showed similar current signals (Figure 30) in different artificial ISF solutions pH values ranging from 6.5 to 8.0, and an RSD of 1.62%.

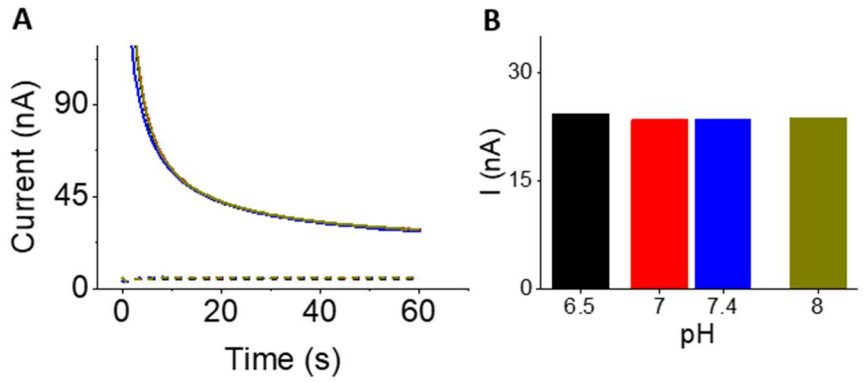

Figure 30: pH analysis via chronoamperometric detection of 2mM BHB in ISF (6.5-8pH)

The resulting chronoamperometric (Figure 31) current response from selectivity analysis and the corresponding relative current response indicated that the potential interferents are negligible compared to the target BHB detection and that the modified MN sensor is selective only for the target analyte and not the common interferences.

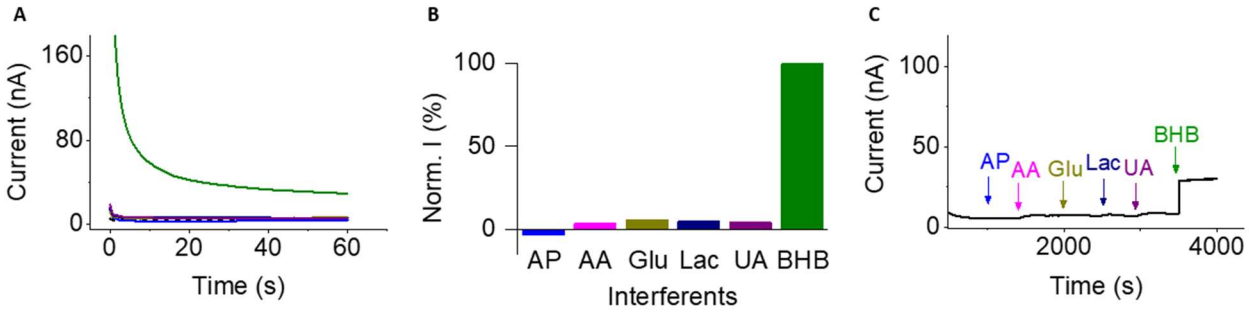

Figure 31: Selectivity analysis via A) chronoamperometric detection of current response of interferents compared to 2mM BHB, B) its corresponding relative current response plot and C) amperometric response of subsequent additions of potential interferents

The resulting curve (Figure 32A) shows 24 repetitive measurements of 2mM BHB concentration at the detection potential of +0.2 V. This data was used to plot a relative current response graph over the 5 h of repetitive testing to show that there is a high stability with a retention

of 92% of the initial current response, and no compromise in the stability of the sensor over extended period of operation (Figure 32B). This is the most critical aspect needed to support on-body testing capabilities.

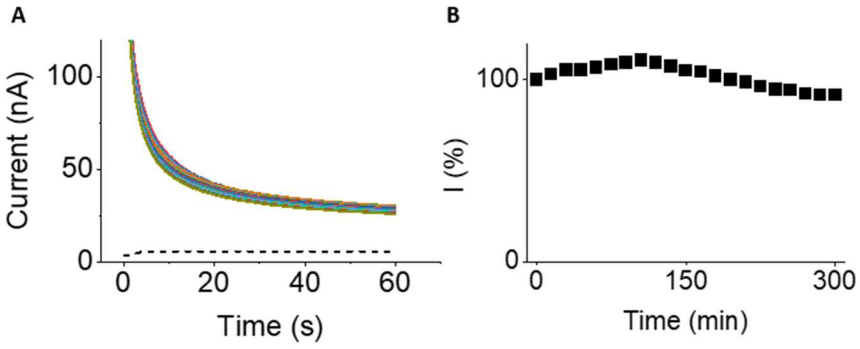

Figure 32: Stability analysis via A) repetitive chronoamperometric detection of 2mM BHB over 5h and B) its corresponding calibration plot

The resulting amperometric plots from the successive addition of 0.5mM BHB in ISF (Figure 33A) and the corresponding calibration plot show that there is a well-defined response and linear trend with similar sensitivity, respectively. The corresponding BHB calibration (Figure 33B) curve was linear over this range (R2 = 0.998). The limit of detection (LOD) was determined to be 95µM. The stability assessment showed high retention of initial current response over the 5h period setting baseline for on-body tests (Figure 33C).

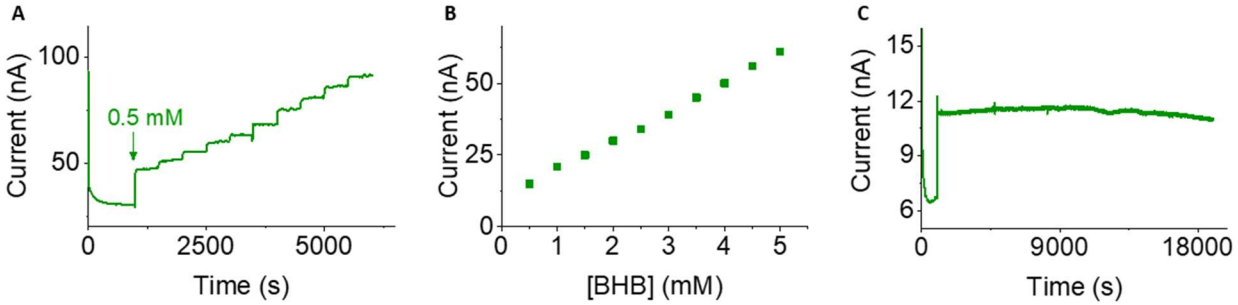

Figure 33: Sensitivity analysis via amperometric detection of successive additions of 0.5mM BHB, its corresponding calibration plot and stability assessment over 5h via amperometric detection of 2mM BHB

The resulting chronoamperogram (Figure 34A) and the relative current response plot (Figure 34B) for the 5 poly-TBO/Au/Pt MNs sensor for reproducibility clearly indicate a very high reproducibility, with a relative standard deviation (RSD) of 2.08%.

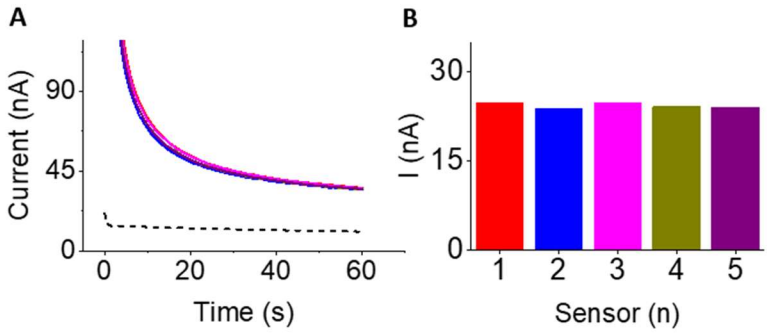

Figure 34: Reproducibility validation via A) chronoamperometric detection of 2mM BHB in 5 enzymatic MN sensors under same conditions and B) the relative current response

The resulting chronoamperogram and the relative current response plot over the 15-day period for shelf-life/storage indicate a good shelf-life with an RSD of 2.87% (Figure 35). The sensor's performance in NADH detection ensures that it can reliably support the specific and sustained monitoring required for accurate ketone measurement on-body.

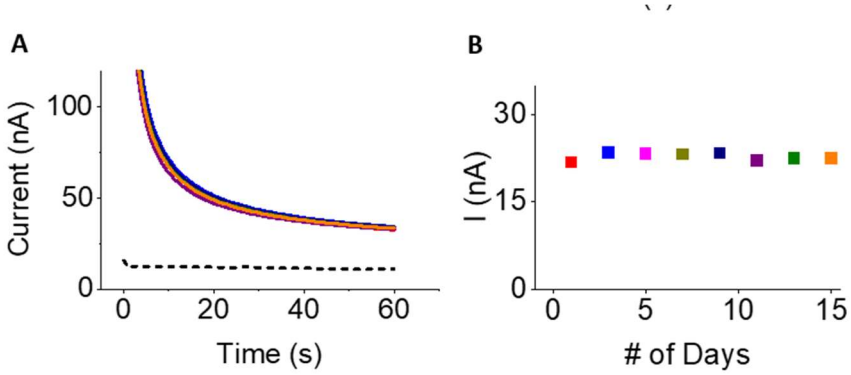

Figure 35: Shelf-life validation via A) chronoamperometric detection of 2mM BHB over different shelf-life periods and B) the relative current response plot

4.4 Cytotoxicity Test

In vitro cytotoxicity assessment (Figure 36) of the microneedle (MN) sensor array, before and after skin penetration, involving co-incubation with the human macrophage cell line (THP-1) for 24 hours. Cell viability was subsequently analyzed using the CellTiter 96 Aqueous One Solution Cell Proliferation Assay (MTS). Within the first 24hrs, no toxic effects were observed, and the cell viability was above 96% in all instances (control, before skin penetration and after skin penetration).

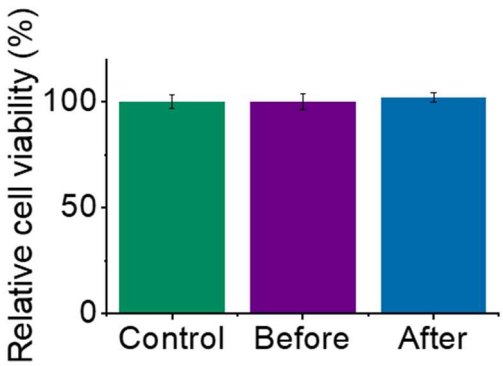

Figure 36: In vitro cytotoxicity assessment of the microneedle (MN) sensor array

4.5 On-body Monitoring of ISF BHB using Wearable MN Sensors

Figures 37A−37D show the real-time amperometric BHB response profiles from the wearable microneedle biosensor, recorded before and after ketone supplementation over 3−4 hours, alongside the corresponding blood BHB profiles. The microneedle current profiles highlight continuous monitoring of the dynamic ISF BHB levels in individual participants. However, a time lag was observed between the ISF and blood BHB profiles, similar to those reported in continuous glucose monitoring (CGM) studies. The data reveal that in all subjects, there was a noticeable increase in the current response within 30−40 minutes after consuming the ketone drink. The results demonstrated a strong correlation between the trends observed in both ISF BHB and blood

BHB profiles, indicating similar temporal patterns in both measurements. The study also revealed individual differences in response times among the subjects. For instance, Participants A-C showed the highest signals within 50 minutes, whereas Participant D exhibited the largest response after 80 minutes. These variations can be attributed to differences in metabolic rates and individual responses to the same ketone drink intake. Additionally, a gradual decline in BHB concentration was observed in all subjects over extended periods, lasting up to 2 hours. It further illustrates the estimated changes in blood BHB concentration profiles for each subject, derived from normalizing the maximum microneedle current response to the peak blood-meter BHB concentration.

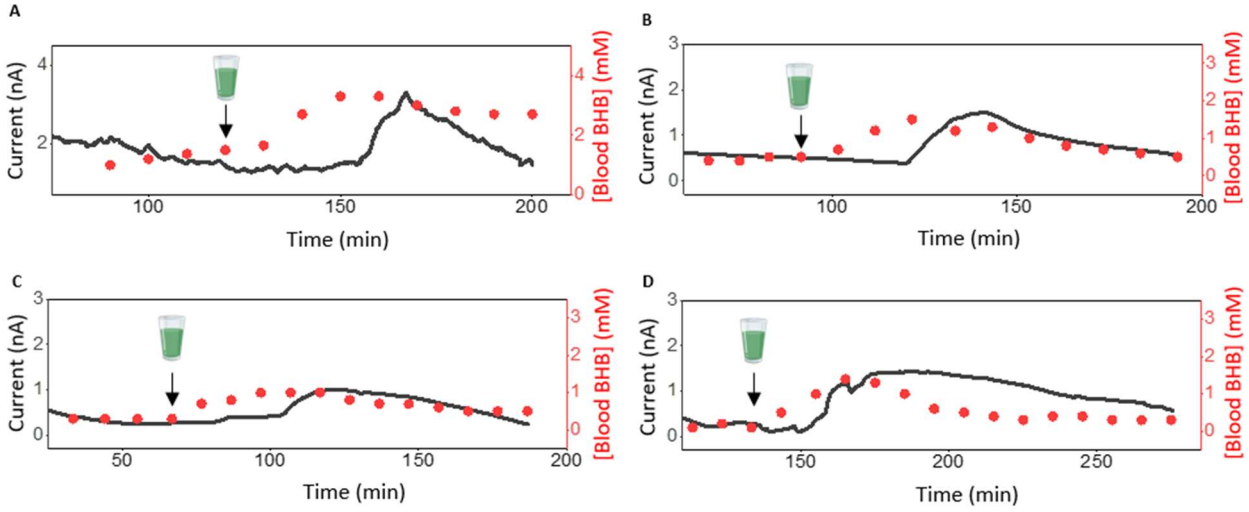

Figure 37: BHB measurements during the consumption of a commercial ketone drink by four healthy human subjects: continuous real-time current response of the MN sensor (black lines) along with the corresponding periodic blood measurements (red dots).

However, a time lag was observed between the ISF and blood BHB profiles, similar to those reported in continuous glucose monitoring (CGM) studies [60] [61]. This delay may result from the physiological time delay caused by the transport of molecules from the bloodstream to the interstitial fluid, influenced by factors such as local blood flow, tissue perfusion, ISF permeability, and local convection. Additionally, technologically induced delays, related to the

inherent lag in electrochemical sensors due to reaction cascades and signal processing, also contribute to this time lag.

The exact cause of these time delays between plasma blood glucose and ISF glucose remains unclear, with studies reporting a wide range of delays from 4 to 50 minutes [60]. Recent glucose tracer experiments using micro-dialysis estimated a physiological delay of about 5−6 minutes. Such delays vary among individuals, regardless of the CGM system used [62] [63] [64]. Literature also suggests that the time delay in adolescents tends to be shorter than in adults and increases with age [65]. In contrast to the well-studied glucose transport, no previous research has explored ketone transport from the vascular compartment to ISF in humans, and thus, there are no established reports on such time delays for BHB.

Compared to traditional CGM technologies, which typically penetrate deeper into the dermis, microneedle-based biosensors, with their shallower penetration, might experience a longer diffusion time in ISF, potentially contributing to the observed time lag. The dehydrogenase-based cascade reaction for BHB detection may also slow down the response time compared to oxidase-based CGM systems. Furthermore, the dynamics between blood and ISF might indicate that capillary barriers between ISF and plasma regions could hinder BHB diffusion. Although BHB is a small biomolecule (0.1 kDa), its movement from blood to ISF may be restricted by the selective barrier of the luminal glycocalyx, which resists negatively charged molecules. Thus, the observed time lag is likely due to the combined effects of these factors impacting BHB partitioning between ISF and blood, as well as the intrinsic delays in the microneedle platform's electrochemical reactions.

Another small experiment that was done to document (Figure 38) the human skin at different times following the removal of the ketone microneedle sensor which shows impact of microneedles on the skin and the indentations over 0min, 10min, 20min, and 30min.

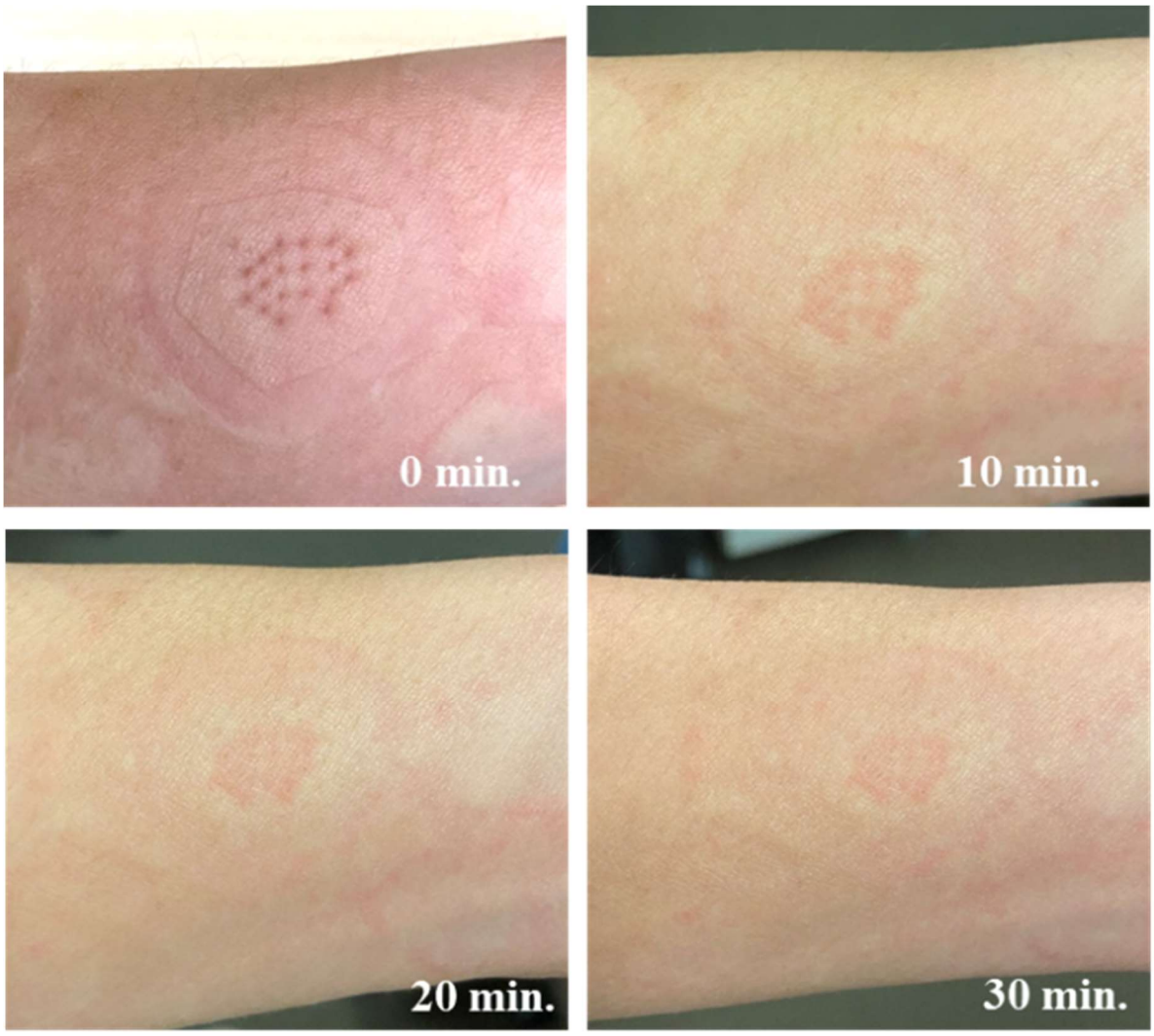

Figure 38: Photographic Documentation Illustrating the Human Skin at Different Times following the Removal of the Ketone Microneedle Sensor.

Chapter 4 is based, in part, on the material as it appears in journal of ACS Sensors, 2024, by Chochanon Moonla, Maria Reynoso, Ana Casanova, An-Yi Chang, Omeed Djassemi, Aishwarya Balaje, Amal Abbas, Zhengxing Li, Kuldeep Mahato, and Joseph Wang. The dissertation author was a co-author of this paper.

Chapter 5 Conclusion

In conclusion, this study successfully addresses the critical need for continuous ketone monitoring by developing an innovative enzymatic electrochemical microneedle-based biosensor. This biosensor enables real-time, minimally invasive tracking of ketones in interstitial fluid, allowing for the accurate measurement of β-hydroxybutyrate following ketone intake, which could lead to the accurate creation of individual BHB profiles. The sensor patch was designed with a focus on ease of assembly, biocompatibility, painless skin penetration, high reliability, and cost-effectiveness which is a significant advancement in the field of continuous monitoring technologies. By integrating poly-TBO and immobilizing HBD/NAD^+, the sensor effectively overcomes challenges related to redox mediator leaching, immobilization of the enzyme, and continuous BHB detection.

Before moving to on-body testing, we conducted extensive in vitro experiments, as detailed in the procedure and results sections. These in vitro studies combined with the cytotoxicity assessment, provided promising results, demonstrating the sensor's effectiveness and reliability, which justified the progression to on-body testing. The practical application of this device was demonstrated through continuous electrochemical monitoring in a small cohort of healthy subjects, where it exhibited a strong correlation between ISF and blood BHB profiles (gold standard finger-pricking blood ketone measurement) over a four-hour monitoring period. These promising results highlight the sensor's potential for accurate and continuous ketone monitoring in real-world settings.

Future work will focus on refining the system by exploring the physiological lag time between blood BHB and microneedle ISF measurements. Developing sophisticated calibration

algorithms to account for this delay will enhance the sensor's precision. Additionally, the integration of glucose monitoring capabilities within the microneedle array is planned, enabling simultaneous tracking of ISF BHB and glucose levels. Further studies will also aim to obtain detailed, context-specific data on BHB diffusion rates through the epidermis to optimize sensor performance. Long-term, this research envisions the integration of wireless electronics and batteries into a single, user-friendly skin-worn patch, enhancing the device’s practicality for everyday use. Extensive clinical trials involving a larger and more diverse population are already underway to validate the sensor's accuracy against gold-standard BHB blood assays and create precise BHB profiles for each individual. This validation would help us move a step closer towards personalized diagnostics and diabetes management. The ultimate goal is to translate this minimally invasive microneedle-based continuous ketone monitoring (CKM) system into a practical tool for routine medical, nutritional, and wellness applications, offering a new standard in personalized healthcare management.

Chapter 6 Bibliography

1 K. K. Dhatariya, N. S. Glaser, E. Codner and G. E. Umpierrez, "Diabetic ketoacidosis," vol. 6, no. 40, 2020.

2 S. L. Kesl, A. M. Poff, N. P. Ward, T. N. Fiorelli, C. Ari, A. J. Van Putten, J. W. Sherwood, P. Arnold and D. P. D'Agostino, "Effects of exogenous ketone supplementation on blood ketone, glucose, triglyceride, and lipoprotein levels in Sprague–Dawley rats," vol. 13, no. 9, 2016.

3 A. Nelson, E. Queathem, P. Puchalska and e. al., "Metabolic Messengers: ketone bodies.," *Nat Metab 5,* p. 2062–2074, 2023.

4 S. Seed, "What Is Ketosis?," WebMD, 11 July 2024. [Online]. Available: https://www.webmd.com/diabetes/what-is-ketosis.

5 J. McIntosh, "What to know about ketosis," Medical News Today, 18 March 2024. [Online]. Available: https://www.medicalnewstoday.com/articles/180858.

6 T. JALILI, Interviewee, *What the Heck is Ketosis?.* [Interview]. 27 September 2022.

7 "Ketosis," wikipedia, 2024. [Online]. Available: https://en.wikipedia.org/wiki/Ketosis.

8 H. Zhu, D. Bi, Y. Zhang and e. al., "Ketogenic diet for human diseases: the underlying mechanisms and potential for clinical implementations.," *Sig Transduct Target Ther,* vol. 7, no. 11, 2022.

9 M. Evans, K. Cogan and B. Egan, "Metabolism of ketone bodies during exercise and training: physiological basis for exogenous supplementation," *The Journal of Physiology,* vol. 595, pp. 2857-2871, 2017.

10 "3-Hydroxybutyrate dehydrogenase," Wikipedia, [Online]. Available: https://en.wikipedia.org/wiki/3-Hydroxybutyrate_dehydrogenase.

11 "β-Hydroxybutyric acid," wikipedia, [Online]. Available: https://en.wikipedia.org/wiki/%CE%92-Hydroxybutyric_acid.

12 M. M. Hoque, S. Shimizu, E. C. Juan, Y. Sato, M. T. Hossain, T. Yamamoto, S. Imamura, K. Suzuki, H. Amano, T. Sekiguchi, M. Tsunoda and A. Takénaka, "Structure of D-3-hydroxybutyrate dehydrogenase prepared in the presence of the substrate D-3-hydroxybutyrate and NAD+.," *Acta Crystallogr Sect F Struct Biol Cryst Commun.,* vol. 65, no. 4, pp. 331-5, 2009.

13 T. M. E. Staff, "Diabetic Ketoacidosis," Merck Manual, Mar 2023. [Online]. Available: https://www.merckmanuals.com/home/quick-facts-hormonal-and-metabolic-disorders/diabetes-mellitus-dm-and-disorders-of-blood-sugar-metabolism/diabetic-ketoacidosis.

14 S. Veneti, M. Grammatikopoulou, E. Kintiraki, G. Mintziori and D. Goulis, "Ketone Bodies in Diabetes Mellitus: Friend or Foe?," *Nutrients,* vol. 15, p. 4383, 2023.

15 S. Raghavan, J. Vassy, Y. Ho, R. Song, D. Gagnon, K. Cho, P. Wilson and L. Phillips, "Diabetes Mellitus–Related All-Cause and Cardiovascular Mortality in a National Cohort of Adults.," *J. Am. Heart Assoc.,* vol. 8, p. e011295, 2019.

16 R. Zhu, S. Zhou, L. Xia and X. Bao, "Incidence, Morbidity and years Lived With Disability due to Type 2 Diabetes Mellitus in 204 Countries and Territories: Trends From 1990 to 2019.," *Front. Endocrinol.,* vol. 13, p. 905538, 2022.

17 "Diabetes," World Health Organization, [Online]. Available: https://www.who.int/news-room/fact-sheets/detail/diabetes. [Accessed 5 April 2023].

18 "Diabetes around the world," IDF Diabetes Atlas, [Online]. Available: https://diabetesatlas.org/.

19 S. C. Team, "Diabetes Statistics," Single Care, 7 June 2024. [Online]. Available: https://www.singlecare.com/blog/news/diabetes-statistics/.

20 "Diabetes and Using Insulin," cdc, [Online]. Available: https://www.cdc.gov/diabetes/php/data-research/index.html#:~:text=1.7%20million%20adults%20aged%2020,1%20diabetes%20and%20using%20insulin.. [Accessed 15 may 2024].

21 C. L. Colvin, O. P. Akinyelure, M. Rajan, M. M. Safford, A. P. Carson, P. Muntner, L. D. Colantonio and L. M. Kern, "Diabetes, gaps in care coordination, and preventable adverse events," *Am J Manag Care,* vol. 29, no. 6, pp. e162-e168, 2023.

22 "Diabetes facts and figures," IDF, [Online]. Available: https://idf.org/about-diabetes/diabetes-facts-figures/. [Accessed 2024].

23 S. Benoit, Y. Zhang, L. Geiss, E. Gregg and A. Albright, "Trends in Diabetic Ketoacidosis Hospitalizations and In-Hospital Mortality — United States, 2000–2014.," *MMWR Morb Mortal Wkly Rep,* p. 67:362–365., 2018.

24 J. Y. Zhang, T. Shang, S. K. Koliwad and D. C. Klonoff, "Continuous Ketone Monitoring: A New Paradigm for Physiologic Monitoring," *J. Diabetes Sci. Technol.,* vol. 15, no. (4), p. 775−780, 2021,.

25 H. Teymourian, C. Moonla, F. Tehrani, E. Vargas, R. Aghavali, A. Barfidokht, T. Tangkuaram, P. P. Mercier, E. Dassau and J. Wang, "Microneedle-Based Detection of Ketone Bodies along with Glucose and Lactate: Toward Real-Time Continuous Interstitial Fluid Monitoring of Diabetic Ketosis and Ketoacidosis.," *Anal. Chem. ,* vol. 92 , no. (2), p. 2291−2300., 2020,.

26 S. Alva, K. Castorino, H. Cho and J. Ou, "Feasibility of Continuous Ketone Monitoring in Subcutaneous Tissue Using a Ketone Sensor," *Diabetes Sci. Technol.,* vol. 15 , no. (4), , p. 768−774., 2021, .

27 H. Teymourian, F. Tehrani, K. Mahato and J. Wang, "Lab under the Skin: Microneedle Based Wearable Devices.," *Adv. Healthc. Mater.,* vol. 10, no. (17), p. No. 2002255., 2021.

28 F. Tasca, C. Tortolini, P. Bollella and R. Antiochia, "Microneedle-Based Electrochemical Devices for Transdermal Biosensing: A Review," *Curr. Opin. Electrochem. ,* vol. 16, p. 42−49., 2019.

29 F. Tehrani, H. Teymourian, B. Wuerstle, J. Kavner, R. Patel, A. Furmidge, R. Aghavali, H. Hosseini-Toudeshki, C. Brown, N. Huang, Z. Patel, P. P. Mercier and J. Wang, "An integrated wearable microneedle array for the continuous monitoring of multiple biomarkers in interstitial fluid," *Nat. Biomed. Eng,* vol. 6, p. 1214–1224 , 2022.

30 Y. Harano, M. Suzuki, H. Kojima, A. Kashiwagi, H. Hidaka and Y. Shigeta, "Development of paper-strip test for 3-hydroxybutyrate and its clinical application," *Diabetes Care,* vol. 7, p. 481e485, 1984.

31 M. Batchelor, M. Green and C. Sketch, "Amperometric assay for the ketone body 3-HYDROXYBUTYRATE," *Anal. Chim. Acta,* vol. 221, pp. 289-294., (1989).

32 N. Forrow, G. Sanghera, S. Walters and J. Watkin, "Development of a commercial amperometric biosensor electrode for the ketone d-3-hydroxybutyrate," *Biosens. Bioelectron.,* vol. 20, pp. 1617-1625, 2005.

33 R. D. Caño, T. Saha, C. Moonla, E. D. l. Paz and J. Wang, "Ketone bodies detection: Wearable and mobile sensors for personalized medicine and nutrition.," *TrAC,* vol. 159, p. 116938, 2023.

34 J. C. Anderson, S. G. Mattar, F. L. Greenway and R. J. Lindquist, "Measuring Ketone Bodies for the Monitoring of Pathologic and Therapeutic Ketosis.," *Obes. Sci. Pract.,* vol. 7, no. (5), p. 646−656., 2021.

35 A. Pfützner, F. Demircik, J. Pfützner, K. Kessler, S. Strobl, J. Spatz, A. Pfützner and A. Lier, "System Accuracy Assessment of a Combined Invasive and Noninvasive Glucometer.," *J Diabetes Sci Technol.,* vol. 14, no. 3, pp. 575-581, 2020.

36 Y. Liu and J. Liu, "Selection of DNA aptamers for sensing uric acid in simulated tears.," *Analysis Sensing ,* vol. 2, no. 4, p. No. e202200010., 2022.

37 C. Moonla, R. D. Caño, K. Sakdaphetsiri, T. Saha, E. D. l. Paz, A. Düsterloh and J. Wang, "Disposable screen-printed electrochemical sensing strips for rapid decentralized measurements of salivary ketone bodies: Towards therapeutic and wellness applications," *Biosens. and Bioelectrons.,* vol. 220, p. 114891, 2023.

38 L. Zheng, D. Zhu, Y. Xiao, X. Zheng and P. Chen, "Microneedle coupled epidermal sensor for multiplexed electrochemical detection of kidney disease biomarkers.," *Biosens. and Bioelectron. ,* vol. 237, p. No. 115506, 2023.

39 J. Huang, A. Yeung, R. Bergenstal, C. K. E. Cengiz, K. Dhatariya, I. Niu, J. Sherr, G. Umpierrez and D. Klonoff, "Update on Measuring Ketones.," *J Diabetes Sci Technol.,* vol. 18, no. 3, pp. 714-726, 2024.

40 L. S. A. M. P. e. a. Vora, "Microneedle-based biosensing.," *Nat Rev Bioeng,* vol. 2, p. 64–81, 2024.

41 C. Moonla, M. Reynoso, A. Casanova, A.-Y. Chang, O. Djassemi, A. Balaje, A. Abbas, Z. Li, K. Mahato and a. J. Wang, "Continuous Ketone Monitoring via Wearable Microneedle Patch Platform," *ACS Sensors,* vol. 9, no. 2, pp. 1004-1013, 2024.

42 "Diabetic ketoacidosis," NHS (UK), 2023. [Online]. Available: https://www.nhs.uk/conditions/diabetic-ketoacidosis/.

43 "Ketones," Cleveland clinic, 2023. [Online]. Available: https://my.clevelandclinic.org/health/body/25177-ketones.

44 G. D. J. Lopaschuk, "Ketones and the cardiovascular system.," *Nat Cardiovasc Res ,* vol. 2, p. 425–437, 2023.

45 J. Sheldon, "Gluconeogenesis," Teach Me Physiology, April 2024. [Online]. Available: https://teachmephysiology.com/biochemistry/atp-production/gluconeogenesis/.

46 S. Watanabe and A. e. a. Hirakawa, "Basic Ketone Engine and Booster Glucose Engine for Energy Production," *Diabetes Research - Open Journal,* vol. 2, pp. 14-23, 2016.

47 C. P. Puchalska P, "Metabolic and Signaling Roles of Ketone Bodies in Health and Disease.," *Annu Rev Nutr. ,* vol. 41, pp. 49-77, 2021 .

48 "Type 1 diabetes," International Diabetes Federation (IDF), [Online]. Available: https://idf.org/about-diabetes/type-1-diabetes/.

49 J. Lizzo, A. Goyal and V. Gupta, "Adult Diabetic Ketoacidosis.," in *StatPearls [Internet]*, Treasure Island (FL), StatPearls Publishing, 2024.

50 "DKA ketoacidosis and ketones," American Diabetes Association, 1995. [Online]. Available: https://diabetes.org/about-diabetes/complications/ketoacidosis-dka/dka-ketoacidosis-ketones. [Accessed 2024].

51 "Biosensor," wikipedia, [Online]. Available: https://en.wikipedia.org/wiki/Biosensor.

52 A. Turner, G. Wilson and I. Kaube, " Biosensors:Fundamentals and Applications.," *Oxford University Press.,* p. p. 770, 1987.

53 J. Wang, Analytical Electroochemistry, John Wiley & Sons, Inc., 2006.

54 A. H. Bretag, *Life Sci.,* vol. 8, p. 319−322, 1969.

55 M. Reynoso, A.-Y. Chang, Y. Wu, R. Murray, S. Suresh, Y. Dugas, J. Wang and N. Arroyo-Currás, "[20]. Reynoso, M.; Chang, A.-Y.; Wu, Y.; Murray, R.; Suresh, S.; Dugas, Y.; Wang, J.; Arroyo-Currás, N. 3D-Printed, Aptamer-Based Microneedle Sensor Arrays Using Magnetic Placement on Live Rats for Pharmacokinetic Measurements in Interstitial Fluid.," *Biosens. Bioelectron.,* Vols. 244, , p. No. 115802., 2024.

56 A.-Y. C. e. a. Maria Reynoso, "3D-printed, aptamer-based microneedle sensor arrays using magnetic placement on live rats for pharmacokinetic measurements in interstitial fluid," *Biosens. and Bioelectrons.,* vol. 244, p. 115802, 2024.

57 B. Prieto-Simón and E. Fàbregas, "Comparative Study of Electron Mediators Used in the Electrochemical Oxidation of NADH.," *Biosens. Bioelectron. ,* vol. 19, no. 10, p. 1131−1138, 2004.

58 C. O. Schmakel, K. S. V. Santhanam and P. J. Elving, "Nicotinamide Adenine Dinucleotide (NAD+) and Related Compounds. Electrochemical Redox Pattern and Allied Chemical Behavior.," *J. Am. Chem. Soc.,* vol. 97, no. 18, p. 5083−5092..

59 Z. Samec and P. J. Elving, "Anodic Oxidation of Dihydronicotinamide Adenine Dinucleotide at Solid Electrodes; Mediation by Surface Species. J. Electroanal. Chem. Interfacial Electrochem.," vol. 144 , no. (1−2),, p. 217−234., 1983, .

60 A. Basu, S. Dube, S. Veettil, M. Slama, Y. C. Kudva, T. Peyser, R. E. Carter, C. Cobelli and R. Basu, "Time Lag of Glucose from Intravascular to Interstitial Compartment in Type 1 Diabetes.," *J. Diabetes Sci. Technol.,* vol. 9, no. 1, p. 63−68, 2015.

61 C. Cobelli, M. Schiavon, C. Dalla Man, A. Basu and R. Basu, "Interstitial Fluid Glucose Is Not Just a Shifted-in-Time but a Distorted Mirror of Blood Glucose: Insight from an in Silico Study.," *Diabetes Technol. Ther. ,* vol. 18 , no. (8), , p. 505−511., 2016,.

62 D. Barry Keenan, J. J. Mastrototaro, S. A. Weinzimer and G. M. Steil, "Interstitial fluid glucose time-lag correction for real-time continuous glucose monitoring.," *Biomed. Signal Process. Control ,* vol. 8, no. 1, p. 81−89, 2013.

63 A. Basu, S. Dube, M. Slama, I. Errazuriz, J. C. Amezcua, Y. C. Kudva, T. Peyser, R. E. Carter, C. Cobelli and R. Basu, "Time lag of glucose from intravascular to interstitial compartment in humans.," *Diabetes ,* vol. 62, no. 12, p. 4083−4087, 2013.

64 G. Schmelzeisen-Redeker, M. Schoemaker, H. Kirchsteiger, G. Freckmann, L. Heinemann and L. Del Re, "Time delay of CGM sensors: relevance, causes, and countermeasures.," *J. Diabetes Sci. Technol.,* vol. 9, no. (5),, p. 1006−1015, 2015.

65 M. Friedel, I. A. Thompson, G. Kasting, R. Polsky, D. Cunningham, H. T. Soh and J. . Heikenfeld, " Opportunities and challenges in the diagnostic utility of dermal interstitial fluid.," *Nat. Biomed. Eng. ,* Vols. 7,, p. 1541−1555., 2023, .